Open access • Posted Content • DOI:10.1101/2021.04.30.442171

Minimal phrase composition revealed by intracranial recordings — **Source link** ⧉

Elliot Murphy, Oscar Woolnough, Patrick S. Rollo, Roccaforte Zj ...+5 more authors

Institutions: University of Texas Health Science Center at Houston, University of Birmingham, Max Planck Society, Memorial Hermann Healthcare System

Topics: Phrase and Middle temporal gyrus

Related papers:

- Time course of semantic processes during sentence comprehension: an fMRI study.

- From letters to composed concepts: A magnetoencephalography study of reading

- Dissociable contributions of frontal and temporal brain regions to basic semantic composition.

- Sentence complexity and input modality effects in sentence comprehension: an fMRI study

- Differential activity in left inferior frontal gyrus for pseudowords and real words: an event-related fMRI study on auditory lexical decision.

Minimal phrase composition revealed by intracranial recordings

Authors:

Elliot Murphy[1,2], Oscar Woolnough[1,2], Patrick S. Rollo[1,2], Zachary Roccaforte[1], Katrien Segaert[3,4], Peter Hagoort[4,5], Nitin Tandon[1,2,6,*]

1. Vivian L. Smith Department of Neurosurgery, McGovern Medical School, University of Texas Health Science Center at Houston, Houston, TX, USA

2. Texas Institute for Restorative Neurotechnologies, University of Texas Health Science Center at Houston, Houston, TX, USA

3. School of Psychology & Centre for Human Brain Health, University of Birmingham, Birmingham, UK

4. Max Planck Institute for Psycholinguistics, Nijmegen, The Netherlands

5. Donders Institute for Brain, Cognition and Behaviour, Nijmegen, The Netherlands

6. Memorial Hermann Hospital, Texas Medical Center, Houston, Texas, USA

*Corresponding author: Nitin Tandon (nitin.tandon@uth.tmc.edu)

Number of figures: 6 (+4 suppl.)

1   **Abstract**

2   The ability to comprehend phrases is an essential component of language. Here we evaluate

3   the neural processes that enable the transition from single word processing to a minimal

4   compositional scheme using intracranial recordings. 19 patients implanted with penetrating

5   depth or surface subdural intracranial electrodes heard auditory recordings of adjective-noun,

6   pseudoword-noun and adjective-pseudoword phrases and judged whether the phrase

7   matched a picture. Stimulus-dependent alterations in broadband gamma power activity (BGA),

8   low frequency power or phase consistency, and phase-locking values across the

9   compositional network were analyzed. The posterior superior temporal sulcus (pSTS) and

10   temporo-occipital junction (TOJ) revealed a fine-structured cortical mosaic, with closely

11   neighboring tissue displaying exclusive sensitivity to either lexicality or phrase structure, but

12   not both. During phrase composition, greater functional connectivity was seen between pSTS-

13   TOJ and both pars triangularis and temporal pole. These two regions also encode anticipation

14   of composition in broadband low frequencies. These results implicate pSTS-TOJ as a crucial

15   hub for the retrieval and computation of minimal phrases. Overall, this work reveals an

16   interface of sparsely interwoven coding for lower and higher level linguistic features, coupled

17   with large-scale network organization, with direct relevance to our understanding of cognitive

18   networks in the human brain.

19   **Keywords**: composition, electrocorticography, semantics, posterior temporal lobe,

20   anticipation, human, language

Introduction

How the brain integrates individual word meanings to comprehend the meaning of multi-word utterances is an issue that has vexed the cognitive neuroscience of language for decades. How the brain computes 'complex meaning' (Hagoort, 2020) from combinations of multiple lexical items is still largely a mystery. This linguistic compositional process – the combination of words into larger structures with new and complex meaning – is also referred to as "Merge" (Chomsky, 1995; Chomsky et al., 2019) or "Unification" (Hagoort, 2013).

The simplest form of studying complex meaning is by using minimal phrases such as in the *red-boat* paradigm, which focuses on simple combinations of two words (Bemis & Pylkkänen, 2011, 2013a; Bozic et al., 2015; Brennan & Pylkkänen, 2012; Flick et al., 2018; Flick & Pylkkänen, 2020; Pylkkänen, 2020; Westerlund et al., 2015; Westerlund & Pylkkänen, 2014), avoiding a range of confounds associated with more complex linguistic stimuli (Berwick, & Stabler, 2019). A "red boat" is interpreted as a boat which is red, and not a red object which hosts boat-related properties, with phrases delivering novel syntactic and conceptual formats (Leivada & Murphy, 2021; Murphy, 2015a; Pietroski, 2018). Experimental work using the *red-boat* paradigm implicates the left anterior temporal lobe (ATL), specifically the temporal pole (Antonucci et al., 2008; Bemis & Pylkkänen, 2011; Lambon Ralph et al., 2012; Pobric et al., 2010; Westerlund & Pylkkänen, 2014; Wilson et al., 2014; Zhang & Pylkkänen, 2018), and posterior temporal regions (Flick & Pylkkänen, 2020; Matchin & Hickok, 2020) as crucial nodes for phrase composition. *Red-boat* experiments isolate semantic composition, which in turn encompasses syntactic composition. These studies report responses that vary in timing (between 180–350ms post-composition) and duration (50–100ms). The left posterior temporal lobe and angular gyrus (AG) also show greater activity for sentences than word lists, and for phrases than words (Brennan et al., 2016; Matchin & Hickok, 2020), making them candidate regions for the retrieval of phrasal templates (Hagoort, 2003, 2017),

Phrase composition is a rapid process that is likely dependent on finely organized sets of distributed cortical substrates. Previous work in the *red-boat* paradigm has been limited by spatiotemporal resolution. Using recordings from intracranial electroencephalography (iEEG) with depth electrodes penetrating grey matter or electrodes located on the cortical surface, we conducted a study of minimal phrase composition with auditory presentations of adjective-noun phrases across a large patient cohort (n = 19).

We utilized grammatical noun phrases ("red boat") and pseudoword phrases with variable positions of the pseudoword ("bleeg boat", "red fulg") to isolate semantic compositional processing. An adjective-pseudoword condition ("red fulg") was included to isolate semantic compositionality and reduce predictability. Given the large number of patients in our study, we

56   were able to analyze not only regions of interest delineated by previous studies, but also a

57   range of temporal, frontal and parietal cortices not previously implicated in models of phrase

58   composition.

59   Studies using scalp electroencephalography and magnetoencephalography (MEG) were used

60   to constrain our analytic space. iEEG provides uniquely high spatiotemporal resolution

61   recordings and is less susceptible to artifacts (e.g., muscle movements) (Arya, 2019; Flinker

62   et al., 2011). High frequency gamma changes (Conner et al., 2019; Forseth et al., 2018;

63   Johnson et al., 2020; Leszczyński et al., 2020; Towle et al., 2008; Yi et al., 2019) typically

64   index local cortical processing and are implicated in a range of cognitive processes (Buzsáki

65   & Watson, 2012; Hovsepyan et al., 2020; Jensen et al., 2019; Marko et al., 2019; Packard et

66   al., 2020; Prystauka & Lewis, 2019). An early anterior negative deflection immediately

67   preceding the critical noun in combinatorial contexts (-50–100ms) (Neufeld et al., 2016) likely

68   indexes syntactic prediction (Lau et al., 2006). Low frequency power increases have also been

69   noted during the anticipatory window (Bastiaansen & Hagoort, 2015; Lewis et al., 2016;

70   Segaert et al., 2018), during phrase composition (Segaert et al., 2018) and in a variety of

71   auditory phrase and sentence processing paradigms (Ding et al., 2016; Keitel et al., 2018;

72   Keitel et al., 2017; Mai et al., 2016). Therefore, we also evaluated the role of low frequencies

73   during anticipatory composition. Lastly, our task required patients to determine whether the

74   words they heard matched a subsequent image, enabling analyses related to phrase-matched

75   and phrase-contrasted contexts.

76

Results

78   Patients were presented with auditory recordings grouped randomly into three conditions:

79   Adjective-Noun, Pseudoword-Noun, Adjective-Pseudoword. A subsequent colored image was

80   presented, and patients were tasked with responding, with a button press, to whether the

81   image matched the phrase or not (Fig. 1A). Across the cohort, we had good coverage over

82   lateral and medial temporal lobe, inferior parietal lobe and inferior frontal regions, with some

83   coverage reaching into other portions of fronto-parietal regions (Fig. 1B). We saw activation

84   in response to the auditory stimuli most prominently in superior and middle temporal regions

85   (Fig. 1C). Below we report results pertaining to lexicality; phrase anticipation; phrase

86   composition; and linguistic-visual unification.

87
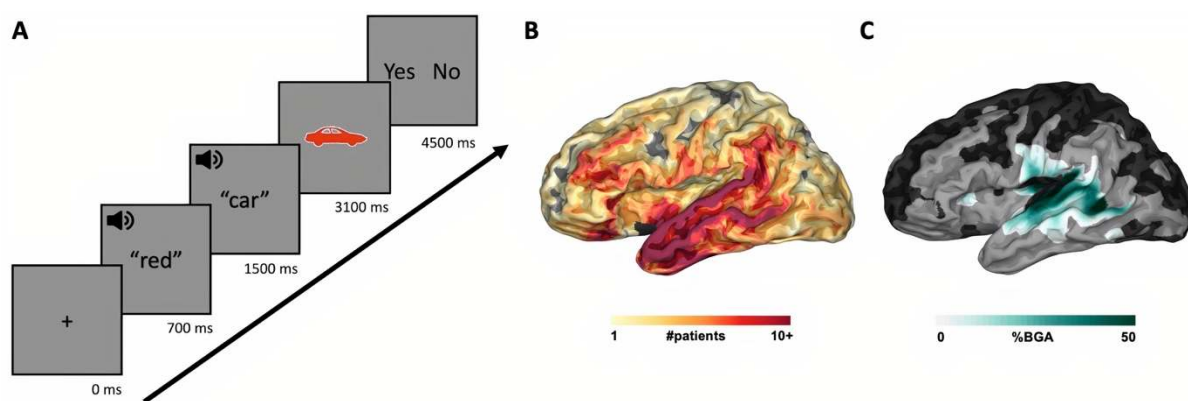
Figure 1: **Experimental paradigm with coverage and activation maps.** (A) Experimental design. Average stimuli length: adjectives (420 ± 39 ms; mean ± SD), nouns (450 ± 75 ms), pseudowords (430 ± 38 ms). (B) Group coverage map of included, left hemisphere electrodes, plotted on a semi-inflated standardised N27 surface. (C) Broadband gamma activity (BGA) increases from baseline (-500 to -100ms prior to first word) for all conditions from 100 to 400ms after onset of the first word (threshold: %BGA > 5%, t > 1.96, patient coverage ≥ 3; *p* < 0.01 corrected). Black surfaces fell below patient coverage threshold.

Behavioral performance

Performance in the image matching task was highly accurate 97 ± 3% (311 ± 11/320 trials) with an average response time of 1599 ± 539 ms. Only correct trials were analyzed further.

Effects of lexicality

To disentangle single word semantic effects from those of combinatorial semantics, we probed the difference in representation of words vs. pseudowords. We generated a surface-based, population-level map of cortical activity using a surface-based mixed-effects multi-level analysis (SB-MEMA) (Conner et al., 2011; Fischl et al., 1999; Kadipasaoglu et al., 2014; Kadipasaoglu et al., 2015), a method specifically designed to account for sampling variations in iEEG and minimize effects of outliers. An SB-MEMA contrasting adjectives vs. pseudowords in word position 1 and nouns vs. pseudowords in word position 2 (Fig. 2A) revealed significantly greater broadband gamma activity (BGA; 70–150 Hz) for pseudowords than words in posterior superior temporal gyrus (pSTG), posterior superior temporal sulcus (pSTS), temporo-occipital junction (TOJ) and pars triangularis 300–700ms after word onset, indexing the additional processing of unfamiliar word sounds in an attempt to derive potential lexicality. The greater BGA increase for pseudowords than words at position 2 than position 1 around

113 pars triangularis and surrounding frontal areas (Fig. 2C), suggests involvement of this region

114 in effortful lexical processing (perhaps in phonological space) to facilitate semantic unification

115 (Hagoort, 2005, 2013; Hagoort & Indefrey, 2014).

116
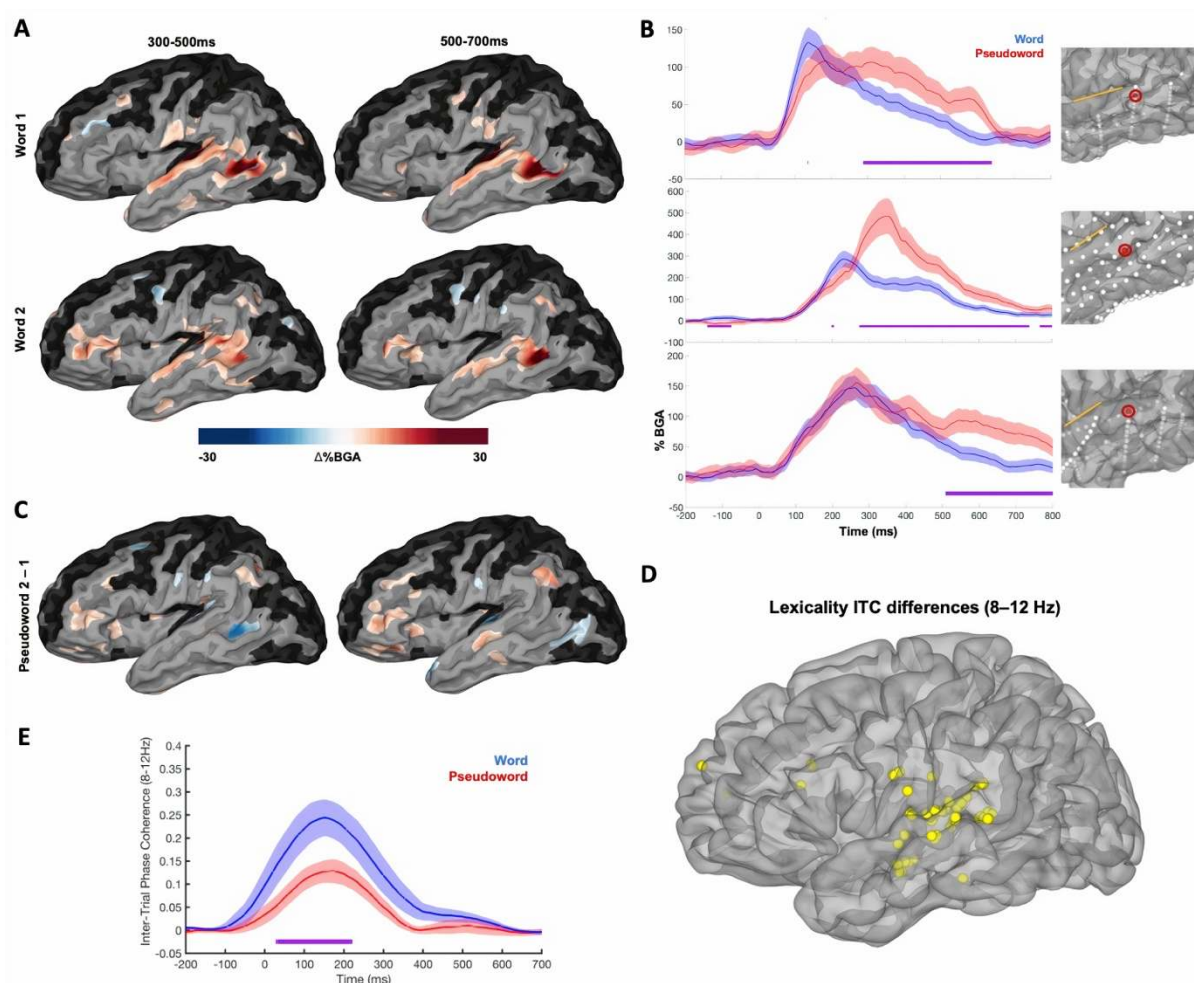
Figure 2: **Grouped analysis for lexicality.** (A) SB-MEMA comparing words vs pseudowords, red colors indexes greater BGA (70–150 Hz) for pseudowords and blue colors for words (threshold: %BGA > 5%, t > 1.96, patient coverage ≥ 3; $p < 0.01$ corrected). Top row: word position 1; bottom row: word position 2. (B) Exemplar electrodes for the words vs pseudowords analysis (red: pseudowords; blue: words). Error bars (colored shading) set at one standard error. Sylvian fissure is marked with a yellow line for reference on each surface. (C) SB-MEMA indicating BGA increases for pseudowords at the second word position relative to pseudowords at the first word position. (D) Electrodes with significant differences in inter-trial phase coherence (ITC) for words vs pseudowords, in posterior temporal cortex (9 patients). (E) ITC in alpha (8–12 Hz) at all electrodes in (D) for words (blue) and pseudowords (red) on the left. T0 = first word onset.

128

129   Additionally, to broaden our assessment of the contributions of lower frequencies, we

130   computed inter-trial phase coherence (ITC) across regions and low frequencies. We found

131   significantly greater ITC values for words relative to pseudowords in and around pSTG (Fig.

132   2D, E; Suppl. Fig. 1) in the alpha band (8–12 Hz). No other ROIs (ATL, pars triangularis, pars

133   orbitalis, MTG, supramarginal gyrus: all FDR-corrected q-values >0.05) displayed such effects

134   for this, or for phrase composition. Alpha phase coherence in pSTG may therefore encode

135   information relevant to lexical interpretation.

136

Compositional anticipation

138   We next contrasted Adjective-Noun and Pseudoword-Noun conditions at the onset of second

139   word presentation, with only the former condition licensing any phrasal anticipation. During

140   the anticipatory window for phrase formation (from -200ms to 0ms prior to the second word

141   onset), low frequency power (8–30 Hz) exhibited an anticipatory effect (Fig. 3). This

142   anticipatory effect was found in IFG, pSTG and ATL, which all appear to be involved in

143   syntactic-semantic prediction generation. In addition, these anticipatory effects were unrelated

144   to BGA, and such widespread, regional effects were not found in delta or theta. For

145   comparison, we also plot the anticipatory window in BGA for -100 to 0ms (Fig. 3B), which

146   exhibited no relation with the lower frequency effects (compare also Fig. 3D with Fig. 3E).

147
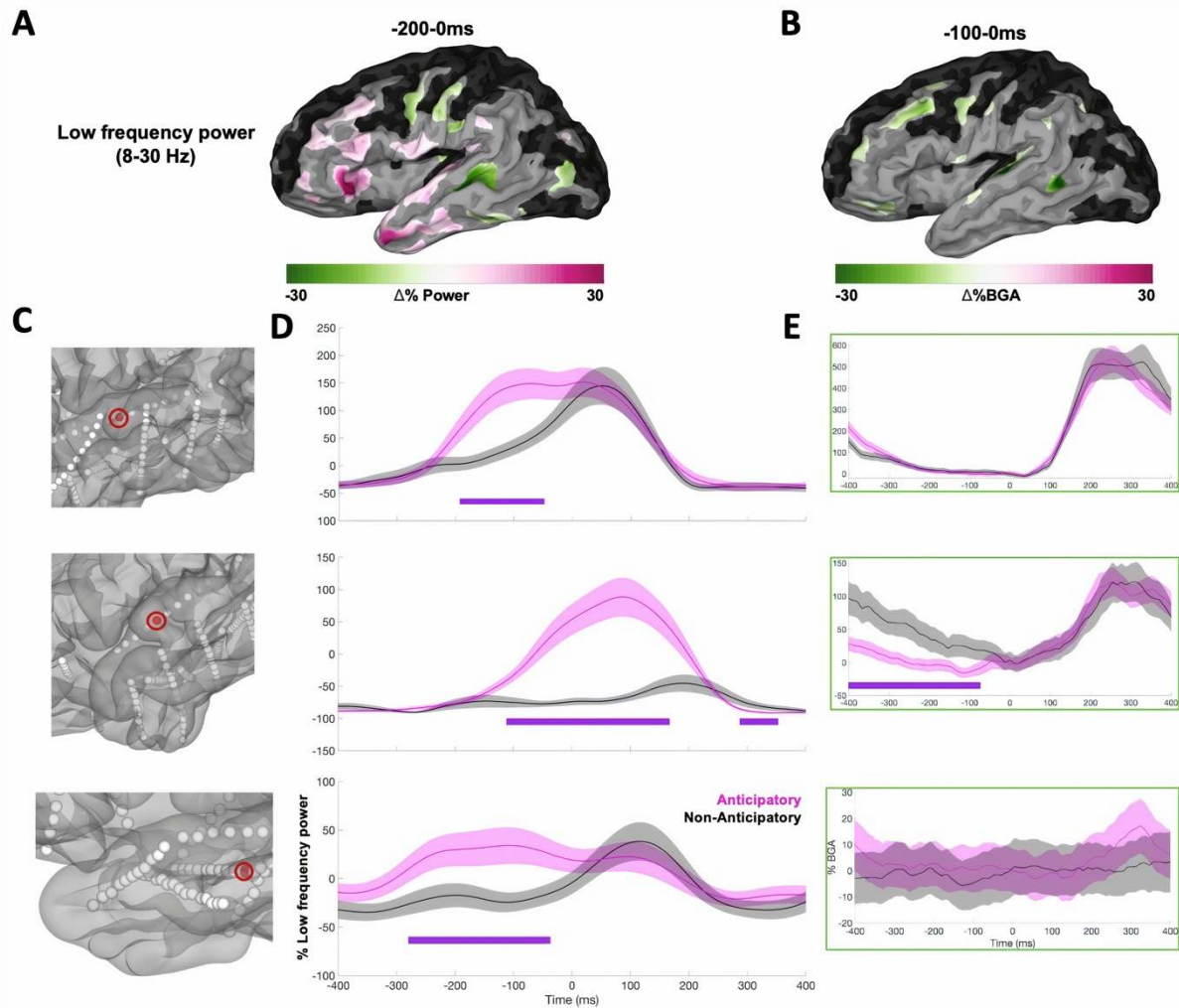
Figure 3: **Syntactic-semantic compositional anticipation.** (A) SB-MEMA for the anticipatory time window centred around second word onset (-200–0ms) for low frequency power. Pink: Greater power for composition anticipation. Green: Greater for no anticipation (i.e. after having heard a Pseudoword at first word position). (B) SB-MEMA for BGA for the same contrast for -100–0ms prior to second word onset. (C)-(E) Exemplar electrodes with location (C), low frequency power traces and (D) BGA traces in dashed green boxes (E), across three patients sorted by row.

155

Phrase composition

The full combinatorial contrast (Adjective-Noun vs [Adjective-Pseudoword + Pseudoword-Noun]), revealed greater BGA for portions of pSTS-TOJ during phrase composition than non-composition (Fig. 4A). The specific onset of this effect was around 210ms after noun onset, with peak BGA at around 300ms (Suppl. Fig. 3). The same region exhibited greater BGA for non-composition at later time points, implicating it in effortful phrase structure derivations.

162   Certain portions of pSTS-TOJ across patients displayed exclusive sensitivity to phrase
163   composition, and not lexicality (Fig. 4B). Other regions – pSTG and inferior frontal gyrus (IFG)
164   – did not show any significant BGA differences between these conditions (Suppl. Fig. 2). Since
165   previous combinatorial effects in phrasal and sentential processing have also localized to
166   anterior temporal pole, we also focused on this region (Suppl. Fig. 2, 4). These portions of left
167   anterior temporal lobe (temporal pole) exhibited increased broadband low frequency activity
168   in response to phrases from approximately 380–460ms and 700–900ms after noun
169   presentation. This activity was unrelated to BGA, indicating that low frequency activity in ATL
170   is an independent component of phrase structure comprehension; likely late-stage semantic
171   processing. The ERPs were dissociable from BGA across the ROIs plotted (Suppl. Fig. 2): A
172   late effect for Non-Composition was found in Broca's area, likely due to greater attempted
173   lexical access for the pseudowords, while a late signature was detected in temporal pole for
174   Composition, potentially related to late-stage conceptual access.
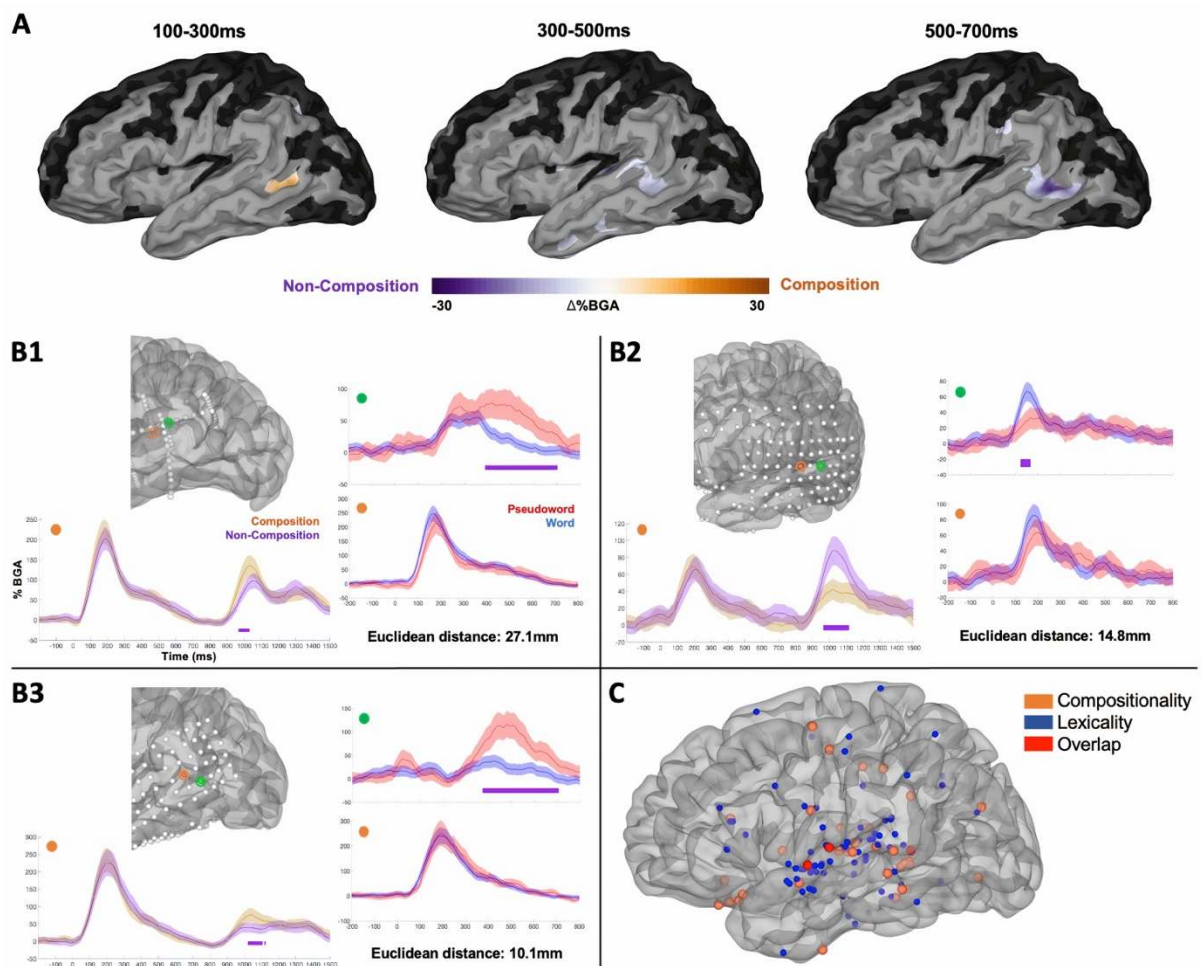

175

176   **Figure 4**: **Grouped analysis for phrase composition.** (A) SB-MEMAs for the phrase
177   composition analysis for BGA. (B) Exemplar electrodes with FDR-corrected (one-tailed t-tests,
178   q<0.05) significance bars in purple plotted in native patient space. Includes compositional

9

179   contrast and lexicality contrast, dissociating neighbouring portions of pSTS-TOJ that
180   responded exclusively for phrase composition and not lexicality (orange dots = composition
181   effect; green dots = lexicality effect). Error bars set at one standard error. Numbers denote
182   distinct patients. (C) Electrodes exhibiting a significant BGA contrast between Compositional
183   and Non-Compositional trials. 39 electrodes (orange) from 12 patients exhibited an FDR-
184   significant contrast (one-tailed t-tests, q<0.05) for compositionality at some point between 0-
185   1000ms after the second word; 97 electrodes across 17 patients for lexicality; 3 electrodes for
186   both across 3 patients.

187

188   Next, we isolated regions of interest to derive cortical functional connectivity during phrase
189   composition. These were based either on results from our main analysis (pSTS-TOJ, temporal
190   pole) or on composition effects described in the literature (inferior frontal regions). To
191   characterize functional connectivity between these regions during phrase composition, we
192   computed phase-locking values (PLV) for electrode pairs situated within pSTS-TOJ with either
193   pars triangularis or anterior temporal lobe. We computed the generalized phase of the
194   wideband filtered (3–50 Hz) signal that has previously been shown to be more effective than
195   the use of narrowband alpha or theta filters (Davis et al., 2020).

196   Among patients with concurrent coverage in pSTS-TOJ and pars triangularis (n = 8, electrode
197   pairs = 231), the majority (n = 5) exhibited significantly greater PLVs for Compositional than
198   for Non-Compositional trials during the 0–500ms period after second word onset, averaging
199   across PLV values for each pair. In patients with joint coverage in pSTS-TOJ and anterior
200   temporal lobe (temporal pole) (n = 8, electrode pairs = 274), the majority (n = 6) showed
201   greater PLVs for the same contrast during the same time window. We plot the magnitude of
202   phase-locking values across these regions and in two exemplar patients (Fig. 5).

10
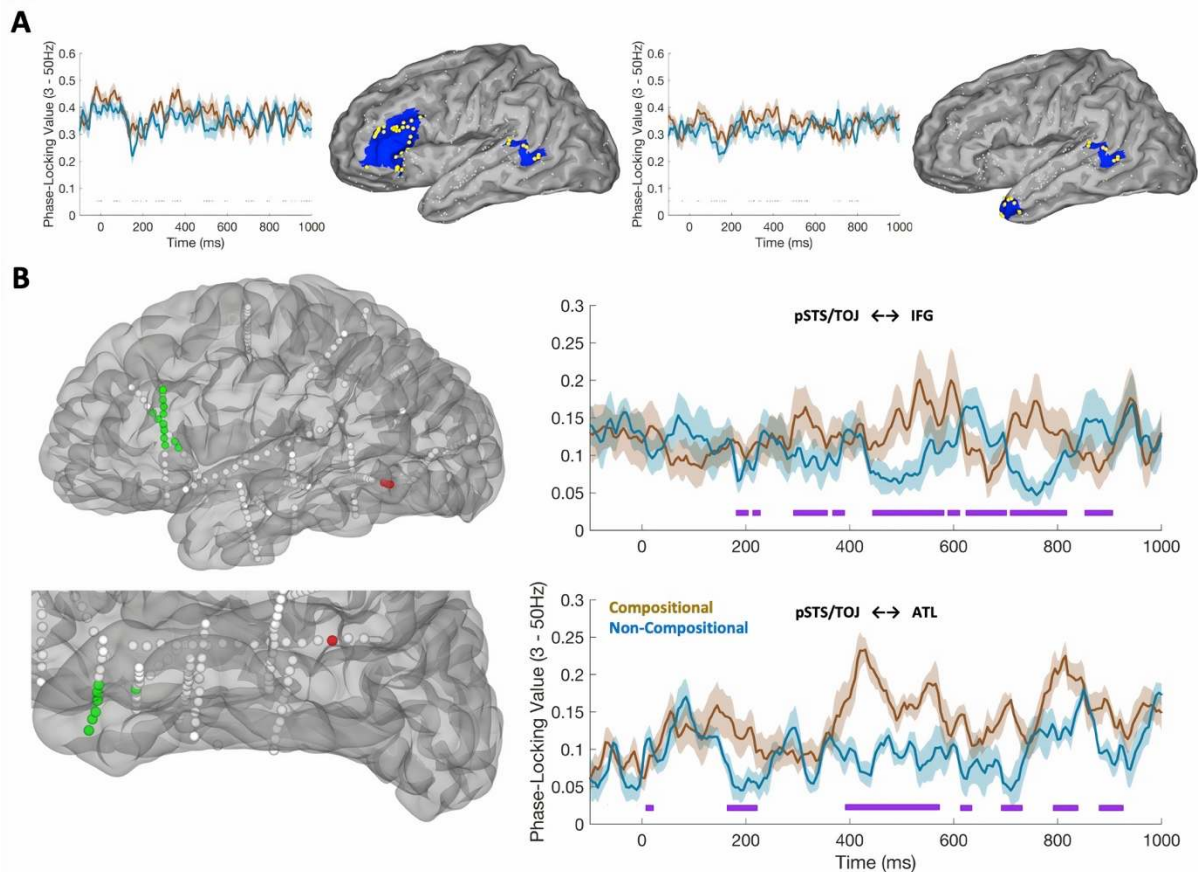
Figure 5: Phase-locking between semantic composition regions of interest. (A) Left: Average generalized phase-locking values (gPLV) for 5 patients showing greater gPLV for phrase composition relative to non-composition between pSTS-TOJ (HCP index: TPOJ1) and pars triangularis (HCP index: 45, IFSa, IFSp, 47l). Right: The same plot but for the 6 patients showing greater gPLV between pSTS-TOJ and temporal pole (HCP index: TGd). (B) Posterior temporal lobe (pSTS-TOJ) gPLVs with inferior frontal gyrus (specifically, pars triangularis) (Top) and anterior temporal lobe (specifically, temporal pole) (Bottom). Left plots show the localization in native space of electrodes significantly involved (q < 0.05) in inter-regional phase-locking (3–50 Hz). Right plots show average time courses (mean ± SEM) of phase-locking value changes from baseline in phrase composition (brown) and non-composition (blue) trials.

Integration of linguistic and visual information

Following each phrase, patients were presented with a matching or non-matching visual representation of the phrase. Comparing the Adjective-Noun trials which contained a matching picture, or a non-matching picture, during the 250–500ms post-picture window, SB-MEMAs revealed two notable effects (Fig. 6): Anterior insula exhibited greater BGA for phrase-picture

11

221   matches, while more dorsal frontal regions, centered around inferior frontal sulcus, exhibited

222   greater BGA for phrase-picture non-matches. Thus, these regions appear to be implicated in

223   linguistic-visual integration and monitoring, likely anchored around the semantic content

224   denoted by both phrases and images and their successful association via some conjunction

225   operator (i.e. [*red* ∧ *boat*], rather than a monadic adjectival or nominal representation). These

226   two regions flank Broca's area, subserving distinct composition-related goals. Since activity of

227   opercular regions can be misattributed to the insula (Woolnough et al., 2019), we ensured that

228   these effects across patients specifically came from electrodes in insula proper, rather than

229   operculum or Broca's area.
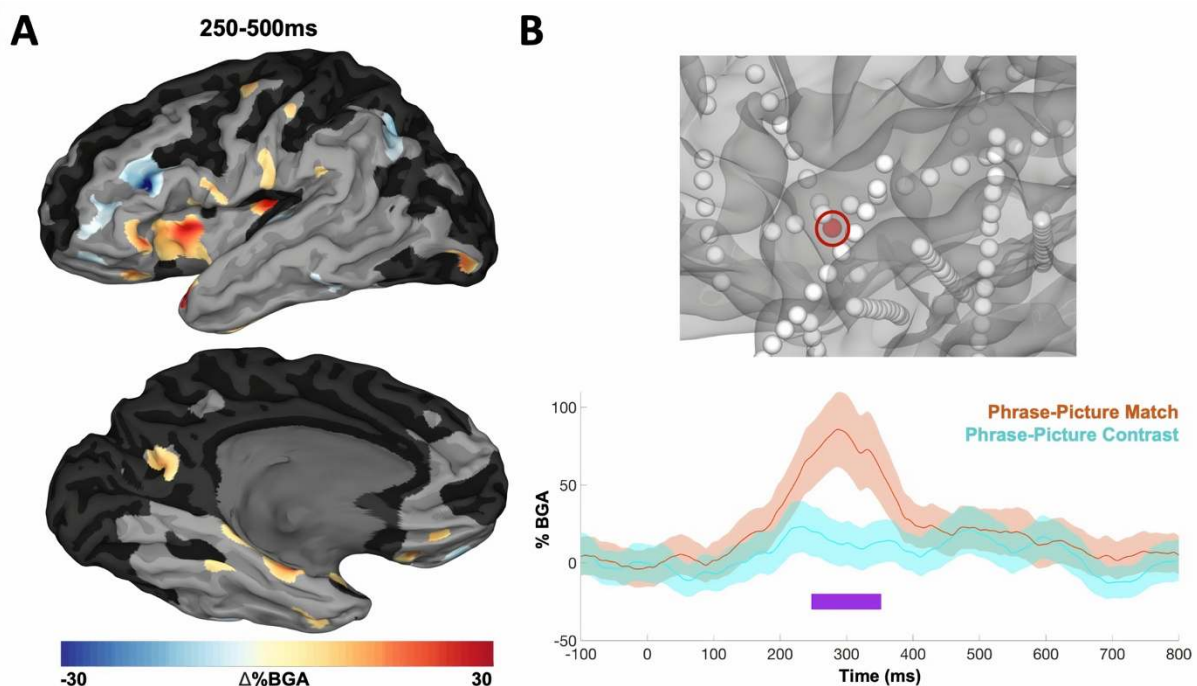
230

231   **Figure 6**: **Grouped analysis for linguistic-visual integration.** (A) SB-MEMA in BGA for

232   phrase-picture match (orange) and phrase-picture contrast (turqoise) increases, 250–500ms

233   after picture onset. (B) Exemplar insula electrode.

234

235   **Discussion**

236   We localized the neural signatures of combinatorial phrase structure comprehension using

237   minimal adjective-noun phrases in a large patient cohort, with both penetrating depth and

238   surface grid intracranial electrodes. We identified a broad portion of posterior temporal cortex

239   as being sensitive to lexicality, and then isolated closely neighboring portions of pSTS-TOJ

240   within patients that responded exclusively to phrase composition, and not lexicality, and vice

241   versa. This computational contrast within a narrow strip of pSTS-TOJ provides a finely

12

242 organized cortical mosaic for the language system (Amunts & Zilles, 2015), going beyond
243 more traditional, broader structure-function mappings for higher-order syntax-semantics. Our
244 results can contribute to the development of a micro-map of pSTS-TOJ with respect to the
245 demands of computational complexity; a necessary step towards understanding the
246 organizational principles of the brain at distinct spatial scales, including ultimately cellular
247 components.

248 Phrase composition was indexed by two main components: Greater BGA in portions of pSTS-
249 TOJ at an early window (around 210-300ms); greater low frequency power in temporal pole
250 at 380–460ms and 700–900ms after the presentation of a phrase-licensing nominal. Greater
251 functional connectivity for phrase composition was found between these regions (pSTS-TOJ
252 and temporal pole) and also between pSTS-TOJ and pars triangularis. pSTS-TOJ is initially
253 active for phrase composition and subsequently shows greater local cortical activity for non-
254 compositional stimuli, indicating its involvement in phrase-related processing. In addition,
255 pSTS-TOJ and pSTG encode local processing of pseudowords, with pSTG likely coding
256 speech signals into articulatory representations (Martin et al., 2019). Anterior portions of IFG
257 exhibit greater BGA for pseudowords at the second word position, possibly indexing increased
258 unification demands with the preceding adjective, compared to a real word (Hagoort, 2005,
259 2013; Hagoort & Indefrey, 2014). This effect may hence index the role of this region in the
260 syntactic and semantic unification of more or less expected continuations, in agreement with
261 earlier results in a sentence context (Hagoort, 2004).

262 In addition, STG, ATL and IFG index composition anticipation in low frequency power,
263 consistent with a predictive neural mechanism for higher-order linguistic information
264 (Bastiaansen & Hagoort, 2015; Benítez-Burraco & Murphy, 2019; Lewis et al., 2016; Murphy,
265 2015b; Prystauka & Lewis, 2019). These anticipatory effects were found in the context of our
266 stimuli being controled for predictability (the addition of the Adjective-Pseudoword condition is
267 the simplest way to achieve this). We additionally showed that alpha phase encodes lexical
268 information exclusively in pSTG via ITC (and not phrase-relevant information).

269 Lastly, anterior insula and inferior frontal sulcus (IFS) subserve the integration of language
270 input with the visual referent. Both of these regions have been argued to be the convergence
271 zones of the ventral (anterior insula) and dorsal (IFS) attentional networks (Cazzoli et al.,
272 2021), while task-evoked pupillary dynamics have been linked to the insula (Kucyi & Parvizi,
273 2020); given current task demands, these dynamics may also underscore our findings.

274 *Lexicality*

275 Our results replicate prior studies in which BGA localized to p/mSTG and pSTS tracks lexicality
276 (Canolty et al., 2007; Humphries et al., 2006; Tanji et al., 2005). In addition, we show

277 recruitment of anterior IFG in this process. Further, pSTG alpha phase coherence may index
278 the coordination of smaller-scale ensembles which may bundle sub-lexical features to yield
279 coherent word-level interpretations of auditory stimuli, in accord with a recent
280 neurocomputational model for lexical feature-set construction (Murphy, 2020).

Anticipatory response

282 According to a range of parsing models (Berwick et al., 2019), adjective-noun syntax is
283 constructed predictively, in anticipation of the noun. Neural response differences in the period
284 preceding the noun in combinatorial trials would likely reflect the generation of this structure.
285 For instance, particular anticipatory amplitude increases have been isolated to the alpha (8–
286 12 Hz) and beta (15–30 Hz) bands in fronto-central and fronto-temporal scalp EEG electrodes,
287 and have been related to the pre-activation of linguistic structure/information (Gastaldon et al.,
288 2020; Segaert et al., 2018). Based on our results, low frequency power in IFG and ATL may
289 be preparing a syntactic slot to be filled by predicted upcoming nominal content, or initiating
290 top-down local coordination of subsequent composition-indexing BGA in pSTS-TOJ. These
291 low frequency dynamics might not even pertain to lexico-semantic prediction specifically, but
292 rather anticipatory stages pertaining to phrasal initiation (Terporten et al., 2019). Our findings
293 are also potentially in line with the notion that beta oscillations can index the construction and
294 maintenance of sentence-level meaning (scaling up from minimal phrases) (Lewis et al.,
295 2016), and the claims that beta can index aspects of syntactic anticipation and phrasal
296 category generation (Benítez-Burraco & Murphy, 2019; Murphy, 2020).

297 Our results may relate to increased recruitment (Bonnefond & Jensen, 2013) of pSTS in late
298 stage lexical processing effort (-200–0ms before the noun). The portion of temporal pole and
299 MTG exhibiting low frequency increases during the anticipatory window could be also involved
300 in late-stage lexico-conceptual processing of adjectival representations, although given the
301 relatively late post-adjective window it is more likely to be related to anticipation. Given
302 increasing evidence for IFG involvement in linear morpho-syntactic processing (Matchin &
303 Hickok, 2020), it is also possible that effects in IFG index a form of lexical anticipation.
304 Predictable word processing specifically pinpoints anterior IFG and ATL in preceding cortical
305 activations (Pulvermüller & Grisoni, 2020). During basic semantic composition, anterior IFG
306 activation has been shown to increase with the amount of lexical information being integrated
307 into the structure (Schell et al., 2017), again pointing to a role for this region as a lexical
308 memory buffer and/or the locus of higher-order predictions.

Minimal phrase composition

310 We found that neighbouring portions of pSTS-TOJ across patients can exclusively code either
311 for lexicality or phrase composition, helping to isolate the core compositional operation in

14

phrase structure generation. While a large area of posterior and superior temporal cortex was sensitive to lexicality, a narrower portion was recruited exclusively to code for phrase structure, generating from simple lexical meanings the more computationally demanding structures of 'complex meaning' (Hagoort, 2020; Pietroski, 2018).

One of the main candidates for phrase composition from previous research, ATL, was implicated via low frequency activity (specifically, temporal pole activity). This may indicate that temporal pole is involved in compositional processing within a noun phrase, with low frequency activity possibly coordinating broader areas in the service of constructing a coherent semantic referent (Wang et al., 2020). Despite ATL being the "most consistent integrative node" (Pylkkänen & Brennan, 2020) in the syntax-semantics combinatorial network, the high spatiotemporal resolution of iEEG presented another candidate for composition: pSTS-TOJ. Increasing morpho-orthographic complexity in a similar minimal phrasal paradigm does not implicate ATL in early processing windows, but seems to delay ATL activity until after intra-word morphological composition (Flick et al., 2018). This suggests that there must be regions independent of semantic and orthographic processing that are common to all forms of (early) phrasal composition. Our findings suggest that pSTS-TOJ might be one such region, although since we only presented auditory stimuli we cannot make any stronger claims. Comparing the discovered composition effect in BGA (Fig. 4A) with the auditory stimuli activation map (Fig. 1C) suggests a clear overlap between sites of initial sensitivity to auditory stimuli and composition-sensitive sites. On the other hand, while there is indeed overlap, there is also a portion of posterior TOJ which seems uniquely active for composition but which is not prominently sensitive to audition, which may point to the involvement of a more modality-independent compositional process. Since MEG cannot detect high frequency activity deep in sulci (Irimia et al., 2012), our iEEG investigation was able to provide new insights here.

With respect to activation timings, we found greater BGA for phrase composition in pSTS-TOJ at 210ms, diminishing around 300ms, after which the majority of responses were greater for non-compositional trials. It is possible that composition-specific computations initiated earlier than this, and that it was only during these time windows that condition differences arose. The later, greater responses for non-composition could be due to more efficient encoding of phrases (hence lower BGA), or, more likely given the latency, late-stage compositional effort/evaluation. It is also possible that the low frequency responses we found to composition in ATL are responses to post-syntactic (pSTS-TOJ) processing, leading to conceptual integration. The timing of these late wrap-up effects might be due to the slow nature of these frequencies and could also be due to some form of traveling oscillatory component (Muller et al., 2018) from posterior temporal areas.

15

347 Our findings are in line with recent models implicating these posterior portions of temporal
348 lobe in phrase structure building (Flick & Pylkkänen, 2020; Law & Pylkkänen, 2021; Matar et
349 al., 2021; Matchin & Hickok, 2020; Murphy, 2018, 2020); a recent meta-analysis of sign
350 language implicating TOJ and pMTG/pSTS in comprehension (Trettenbrein et al., 2020); and
351 the finding that cross-linguistic (French and Chinese) reading competence is linked to pSTS
352 (Feng et al., 2020), contributing to the neural localization of complex composition (Chomsky
353 et al., 2019; Pietroski, 2018). In particular, evidence from neuroimaging and lesion-deficit
354 mapping indicates a role for pMTG in syntactic comprehension and production (Matchin &
355 Hickok, 2020), while pSTS has been implicated via iEEG in hierarchical syntactic
356 computations (Nelson et al., 2017). Data from brain stimulation implicate postero-middle
357 temporal areas in syntactic processing (Duffau et al., 2014), and a recent *red-boat* study in
358 fMRI implicated a broad portion of pMTG in meaningful phrase composition (Graessner et al.,
359 2021). Impairments in grammaticality judgments have primarily been linked to posterior
360 temporal lobe damage (Wilson & Saygin, 2004). Lastly, widespread monotonic fronto-
361 temporal language network gamma power increases over the course of sentence reading
362 have been documented in iEEG (Fedorenko et al., 2016); our findings isolate a more specific
363 site in the network responsible for the core compositional operator underlying sentence
364 comprehension.

365 We also discovered greater functional connectivity between pSTS-TOJ and both temporal
366 pole and pars triangularis after the presentation of the phrase-licensing nominal (Fig. 5). White
367 matter atlas consultation reveals that the subcortical distribution of responses to semantic
368 stimuli reflects the continuous and homogenous ventral course of functional information in the
369 deep white matter of the temporal lobe, from TOJ, ascending to white matter underneath the
370 posterior two-thirds of IFG (Sarubbo et al., 2020). These ventral workflow pathways subserve
371 our regions of interest (temporal pole; TOJ; IFG). In addition, arcuate fasciculus is classically
372 implicated in connectivity between pSTS-TOJ and pars triangularis (Figley et al., 2017;
373 Glasser & Rilling, 2008). In relation to current findings and frameworks, it is possible that the
374 formation of phrase structure in pSTS-TOJ feeds categorial information (e.g. phrase type) to
375 interpretation interfaces in ATL and memory/control interfaces in pars triangularis (a form of
376 "spell-out"). One such piece of information encoded via PLV would be the phrase
377 category/label (Adger, 2012; Murphy, 2015a; Murphy & Shim, 2020). These results may point
378 to a degree of top-down control from pars triangularis on initial phrase construction in pSTS-
379 TOJ (Hagoort et al., 2009). The more precise computational role of such connectivity metrics
380 requires further empirical, and conceptual, advances.

381 Inhibition of a portion of left posterior temporal lobe (pSTS, pSTG and temporo-parietal
382 junction) selectively impairs the ability to produce appropriate functional morphemes for

16

383   particular hierarchical relations, but does not effect any other sub-linguistic process such as
384   semantic or lexical retrieval (Lee et al., 2018). Our data are compatible with the idea that in
385   connection with other areas, such as IFG (Baggio & Hagoort, 2011; Zaccarella et al., 2021),
386   pSTS-TOJ contributes to both morphological and phrasal unification (Jackendoff & Audring,
387   2020; Rizzi, 2016). Our results are concordant with a division between sensitivity to non-local
388   dependency structure (in left anterior temporal pole and IFG) and sensitivity to phrase
389   structure (in left pSTG) (Lopopolo et al., 2021). Data from sEEG comparing noun phrases and
390   acoustically-matched, identical words acting as verb phrases (with the latter demanding richer
391   syntactic structure) reveals greater high gamma activity in MTG and STG in the coding of
392   complex syntax (Artoni et al., 2020). This points to partial spatial overlap with our composition
393   effects, in compliance with the idea that the re-application of recursive hierarchical structure
394   generation calls upon the same basic compositional operator (i.e., that the computation
395   implicated in forming verb phrases is the same operation that forms "red boat").

396   While we did not find composition effects in inferior parietal lobule (in particular, angular gyrus),
397   and had good electrode coverage here, this may be due to this region's role in higher-order
398   semantic processing (e.g. thematic role assignment, discourse structure) and event structure
399   (Boylan et al., 2015). For instance, there is a range of evidence, including from intracranial
400   recordings, that taxonomic conceptual relationships are encoded in ATL, while thematic
401   relationships are encoded in angular gyrus (Davis & Yee, 2019; Thye et al., 2021).

402   Given the nature of our stimuli, we can make direct claims about semantic composition, and
403   we suspect that portions of pSTS-TOJ are also implicated in minimal syntax, however the
404   dynamics of the syntax network may differ from that of the semantic compositional network.
405   Overall, our results contribute to isolating the neural signatures of basic phrase structure
406   composition, an elementary computational procedure of natural language and potentially a
407   species-defining property (Friederici et al., 2017; Murphy, 2019; Murphy et al., 2021), and we
408   hope that future intracranial research can expand on our findings.

409

410   **Materials and Methods**

411   _Participants_: 19 patients (10 male, 18-41 years, IQ 97 ± 12, 2 left-handed) participated in the
412   experiment after written informed consent was obtained. All were native English speakers. All
413   experimental procedures were reviewed and approved by the Committee for the Protection of
414   Human Subjects (CPHS) of the University of Texas Health Science Center at Houston as
415   Protocol Number HSC-MS-06-0385.

416 *Electrode Implantation and Data Recording*: Data were acquired from either subdural grid
417 electrodes (SDEs; 6 patients) or stereotactically placed depth electrodes (sEEGs; 12 patients)
418 (Fig. 1B). SDEs were subdural platinum-iridium electrodes embedded in a silicone elastomer
419 sheet (PMT Corporation; top-hat design; 3mm diameter cortical contact), and were surgically
420 implanted via a craniotomy (Conner et al., 2011; Pieters et al., 2013; Tandon, 2012; Tong et
421 al., 2020). sEEGs were implanted using a Robotic Surgical Assistant (ROSA; Medtech,
422 Montpellier, France) (Rollo et al., 2020; Tandon et al., 2019). Each sEEG probe (PMT
423 corporation, Chanhassen, Minnesota) was 0.8mm in diameter and had 8-16 electrode
424 contacts. Each contact was a platinum-iridium cylinder, 2.0mm in length and separated from
425 the adjacent contact by 1.5-2.43mm. Each patient had 12-20 such probes implanted.
426 Following surgical implantation, electrodes were localized by co-registration of pre-operative
427 anatomical 3T MRI and post-operative CT scans in AFNI (Cox, 1996). Electrode positions
428 were projected onto a cortical surface model generated in FreeSurfer (Dale et al., 1999), and
429 displayed on the cortical surface model for visualization (Pieters et al., 2013). Intracranial data
430 were collected during research experiments starting on the first day after electrode
431 implantation for sEEGs and two days after implantation for SDEs. Data were digitized at 2 kHz
432 using the NeuroPort recording system (Blackrock Microsystems, Salt Lake City, Utah),
433 imported into Matlab, initially referenced to the white matter channel used as a reference for
434 the clinical acquisition system and visually inspected for line noise, artifacts and epileptic
435 activity. Electrodes with excessive line noise or localized to sites of seizure onset were
436 excluded. Each electrode was re-referenced to the common average of the remaining
437 channels. Trials contaminated by inter-ictal epileptic spikes, saccade artefacts and trials in
438 which participants responded incorrectly were discarded.

439 *Stimuli and Experimental Design*: Participants were presented with two-word auditory
440 phrases, grouped by three conditions: Adjective-Noun ("red boat"), Adjective-Pseudoword
441 ("red neub"), Pseudoword-Noun ("zuik boat"). Since these pseudoword phrases include
442 phonologically viable nonwords, differences in the second position of the phrase between
443 these items and the grammatical noun phrases are likely a result of compositional processing.
444 While most previous studies have presented a licensable noun, our inclusion of the Adjective-
445 Pseudoword condition further isolates composition and reduces predictability. To ensure
446 attention was maintained, after each trial participants were shown a colored drawing and
447 asked to press a button indicating whether the picture matched the phrase they had just heard.
448 Participants were told to respond positively only when the picture fully matched the phrase
449 (e.g. the phrase "red boat" followed by a picture of a red car, or a blue boat, would be negative).
450 Auditory and visual stimuli were recruited from previous *red-boat* experiments (Bemis &
451 Pylkkänen, 2013b).

452　A fixation cross was presented in the centre of the screen for 700ms followed by the first word
453　and 800ms later the second word was presented. 1600ms after the onset of the second word
454　the picture was presented, and 1400ms after picture presentation participants were prompted
455　to respond (Fig. 1A). Following their response, a blank screen was shown for 1500ms. Stimuli
456　were presented in a pseudorandom order, with no repetition amongst items. The number of
457　trials per block across the full experiment was as follows: Adjective-Noun (80), Pseudoword-
458　Noun (40), Adjective-Pseudoword (40). All patients undertook 2 blocks. Half of the Adjective-
459　Noun trials matched the picture presented (i.e. "red boat" was heard by the patient, and a
460　picture of a red boat was then presented), and the other half did not match. 6 adjectives were
461　used: black, blue, brown, green, pink, red (length M: 4.3, SD: 0.7; SUBTLEXus log-frequency
462　3.64). 20 nouns were used: bag, bell, boat, bone, cane, cross, cup, disc, flag, fork, hand, heart,
463　house, key, lamp, leaf, lock, plane, shoe, star (length M: 4.0, SD: 0.6; log-frequency 3.38)
464　(Brysbaert, New, & Keuleers, 2012). 6 pseudowords were used: beeg, cresp, kleg, nar, neub,
465　zuik (length M: 4.0, SD: 0.6). Average stimuli length: Adjectives (420 ms), Nouns (450 ms),
466　Pseudowords (430ms).

467　Stimuli were presented using Psychtoolbox (Kleiner et al., 2007) on a 15.4" LCD screen
468　positioned at eye-level, 2-3' from the patient. Auditory stimuli were presented using stereo
469　speakers (44.1 kHz, MacBook Pro 2015).

470　*Signal Analysis*: A total of 3458 electrode contacts were implanted in these patients; 2135 of
471　these were included for analysis after excluding channels proximal to the seizure onset zone
472　or exhibiting excessive inter-ictal spikes or line noise. Analyses were performed by first
473　bandpass filtering the raw data of each electrode into broadband gamma activity (BGA; 70–
474　150 Hz) following removal of line noise and its harmonics (zero-phase 2nd order Butterworth
475　band-stop filters). Electrodes were also visually inspected for saccade artefacts. A frequency
476　domain bandpass Hilbert transform (paired sigmoid flanks with half-width 1.5 Hz) was applied
477　and the analytic amplitude was smoothed (Savitzky-Golay FIR, 3rd order, frame length of
478　251ms; Matlab 2019b, Mathworks, Natick, MA). BGA was defined as percentage change from
479　baseline level; -500 to -100ms before the presentation of the first word in each trial. Periods
480　of significant activation were tested using a one-tailed t-test at each time point and were
481　corrected for multiple comparisons with a Benjamini-Hochberg false detection rate (FDR)
482　threshold of $q<0.05$. For the grouped analysis, all electrodes were averaged within each
483　subject and then the between-subject averages were used.

484　To provide statistically robust and topologically precise estimates of BGA, and to account for
485　variations in sampling density, population-level representations were created using surface-
486　based mixed-effects multilevel analysis (SB-MEMA) (Conner et al., 2011; Fischl et al., 1999;

Kadipasaoglu et al., 2014; Kadipasaoglu et al., 2015). This method accounts for sparse sampling, outlier inferences, as well as intra- and inter-subject variability to produce population maps of cortical activity. A geodesic Gaussian smoothing filter (3mm full-width at half-maximum) was applied. Significance levels were computed at a corrected alpha-level of 0.01 using family-wise error rate corrections for multiple comparisons. The minimum criterion for the family-wise error rate was determined by white-noise clustering analysis (Monte Carlo simulations, 5000 iterations) of data with the same dimension and smoothness as that analyzed (Kadipasaoglu et al., 2014). Results were further restricted to regions with at least three patients contributing to coverage and BGA percent change exceeding 5%.

Anatomical groups of electrodes were delineated, firstly, through indexing electrodes to the closest node on the standardized cortical surface (Saad & Reynolds, 2012), and secondly, through grouping channels into parcellations determined by Human Connectome Project (HCP) space (Glasser et al., 2016). Parametric statistics were used since HCP regions of interest contained >30 electrodes. When contrasting experimental conditions, two-sided paired t-tests were evaluated at each time point for each region and significance levels were computed at q<0.01 using an FDR correction for multiple comparisons.

To generate event-related potentials (ERPs), the raw data were band pass filtered (0.1–50 Hz). Trials were averaged together and the resultant waveform was smoothed (Savitzky-Golay FIR, third-order, frame length of 251ms). To account for differences in polarity between electrodes, ERPs were converted to root mean square (RMS), using a 50ms sliding window. All electrodes were averaged within each subject, within ROI, and then the between subject averages were used.

There is increasing evidence that the phase of activation across distributed neural populations correlates with distinct underlying neural processes from the amplitude (Buzsáki, 2019; Fries, 2015; Sauseng & Klimesch, 2008). We investigated the influence of lexicality and phrase construction on inter-trial phase coherence (ITC). Phase information was extracted from the band-pass filtered data (zero-phase 3rd order Butterworth band-pass filter) using a Hilbert transform. ITC was calculated as the circular mean (absolute vector length) of instantaneous phase of stimulus-aligned trials computed as the median value of 10 iterations of a random 50% of trials.

To explore the functional connectivity between regions of interest, we used a generalized phase-locking analysis to estimate the dominant spatio-temporal distributions of field activity, and the strength of the coupling between them. Phase information was extracted from the down-sampled (200 Hz) and wide band-pass filtered data (3–50 Hz; zero-phase 8th order Butterworth band-pass filter) using the 'generalized phase' method (Davis et al., 2020) with a

single-sided Fourier transform approach (Marple, 1999). This method captures the phase of the predominant fluctuations in the wideband signal and minimizes filter-related distortion of the waveform. PLV was calculated as the circular mean (absolute vector length) of the instantaneous phase difference between each electrode pair at each time point and baselined to the period -500 to -100 ms before onset of the first word. Statistics were calculated using the mean PLV of correctly answered trials between 0 to 500ms after second word onset, comparing against a null distribution generated by randomly re-pairing trial recordings across the electrode pairs 500 times. Significant PLV was accepted at a threshold of $p < 0.05$.

Acknowledgements

References

Adger, D. (2012). *A Syntax of Substance*. https://doi.org/10.7551/mitpress/9780262018616.001.0001

Amunts, K., & Zilles, K. (2015). Architectonic Mapping of the Human Brain beyond Brodmann. *Neuron*, *88*(6), 1086–1107. https://doi.org/10.1016/j.neuron.2015.12.001

Antonucci, S., Beeson, P., Labiner, D., & Rapcsak, S. (2008). Lexical retrieval and semantic knowledge in patients with left inferior temporal lobe lesions. *Aphasiology*, *22*(3), 281–304. https://doi.org/10.1080/02687030701294491

Artoni, F., D'Orio, P., Catricalà, E., Conca, F., Bottoni, F., Pelliccia, V., … Moro, A. (2020). High gamma response tracks different syntactic structures in homophonous phrases. *Scientific Reports*, *10*(1), 7537. https://doi.org/10.1038/s41598-020-64375-9

Arya, R. (2019). Similarity of spatiotemporal dynamics of language-related ECoG high-gamma modulation in Japanese and English speakers. *Clinical Neurophysiology*, *130*(8), 1403–1404. https://doi.org/10.1016/j.clinph.2019.05.006

Baggio, G., & Hagoort, P. (2011). The balance between memory and unification in semantics: A dynamic account of the N400. *Language and Cognitive Processes*, *26*(9), 1338–1367. https://doi.org/10.1080/01690965.2010.542671

Bastiaansen, M., & Hagoort, P. (2015). Frequency-based Segregation of Syntactic and Semantic Unification during Online Sentence Level Language Comprehension. *Journal of Cognitive Neuroscience*, *27*(11), 2095–2107. https://doi.org/10.1162/jocn_a_00829

Bemis, D. K., & Pylkkänen, L. (2013). Basic linguistic composition recruits the left anterior temporal lobe and left angular gyrus during both listening and reading. *Cerebral Cortex*. https://doi.org/10.1093/cercor/bhs170

Bemis, Douglas K., & Pylkkänen, L. (2011). Simple composition: A magnetoencephalography investigation into the comprehension of minimal linguistic phrases. *Journal of Neuroscience*, *31*(8), 2801–2814. https://doi.org/10.1523/JNEUROSCI.5003-10.2011

Bemis, Douglas K., & Pylkkänen, L. (2013). Combination across domains: An MEG investigation into the relationship between mathematical, pictorial, and linguistic processing. *Frontiers in Psychology, 3*, 583. https://doi.org/10.3389/fpsyg.2012.00583

Benítez-Burraco, A., & Murphy, E. (2019). Why Brain Oscillations Are Improving Our Understanding of Language. *Frontiers in Behavioral Neuroscience*. https://doi.org/10.3389/fnbeh.2019.00190

570   Berwick, R. C., Stabler, E. P., Berwick, R. C., & Stabler, E. P. (2019). Minimalist parsing. In *Minimalist Parsing*.

571   https://doi.org/10.1093/oso/9780198795087.003.0001

572   Boylan, C., Trueswell, J. C., & Thompson-Schill, S. L. (2015). Compositionality and the angular gyrus: A multi-

573   voxel similarity analysis of the semantic composition of nouns and verbs. *Neuropsychologia*, *78*, 130–141.

574   https://doi.org/10.1016/j.neuropsychologia.2015.10.007

575   Bozic, M., Fonteneau, E., Su, L., & Marslen-Wilson, W. D. (2015). Grammatical analysis as a distributed

576   neurobiological function. *Human Brain Mapping*, *36*(3), 1190–1201. https://doi.org/10.1002/hbm.22696

577   Brennan, J., & Pylkkänen, L. (2012). The time-course and spatial distribution of brain activity associated with

578   sentence processing. *NeuroImage*, *60*(2), 1139–1148. https://doi.org/10.1016/j.neuroimage.2012.01.030

579   Brennan, J. R., Stabler, E. P., Van Wagenen, S. E., Luh, W. M., & Hale, J. T. (2016). Abstract linguistic structure

580   correlates with temporal activity during naturalistic comprehension. *Brain and Language*, *157–158*, 81–94.

581   https://doi.org/10.1016/j.bandl.2016.04.008

582   Brysbaert, M., New, B., & Keuleers, E. (2012). Adding part-of-speech information to the SUBTLEX-US word

583   frequencies. *Behavior Research Methods*, *44*(4), 991–997. https://doi.org/10.3758/s13428-012-0190-4

584   Buzsáki, G. (2019). *The Brain from Inside Out*. https://doi.org/10.1093/oso/9780190905385.001.0001

585   Buzsáki, G., & Watson, B. O. (2012). Brain rhythms and neural syntax: implications for efficient coding of

586   cognitive content and neuropsychiatric disease. *Dialogues in Clinical Neuroscience*, *14*(4), 345–367.

587   https://doi.org/10.31887/DCNS.2012.14.4/gbuzsaki

588   Canolty, R. T., Soltani, M., Dalal, S. S., Edwards, E., Dronkers, N. F., Nagarajan, S. S., … Knight, R. T. (2007).

589   Spatiotemporal Dynamics of Word Processing in the Human Brain. *Frontiers in Neuroscience*, *1*(1), 185–

590   196. https://doi.org/10.3389/neuro.01.1.1.014.2007

591   Cazzoli, D., Kaufmann, B. C., Paladini, R. E., Müri, R. M., Nef, T., & Nyffeler, T. (2021). Anterior insula and

592   inferior frontal gyrus: where ventral and dorsal visual attention systems meet. *Brain Communications*.

593   https://doi.org/10.1093/braincomms/fcaa220

594   Chomsky, N. (1995). *The Minimalist Program*. Cambridge, MA: MIT Press.

595   Chomsky, N., Gallego, A. J., & Ott, D. (2019). Generative grammar and the faculty of language: insights,

596   questions, and challenges. *Catalan Journal of Linguistics Special Issue*, 226–261.

597   Conner, C. R., Ellmore, T. M., Pieters, T. A., di Sano, M. A., & Tandon, N. (2011). Variability of the relationship

598   between electrophysiology and BOLD-fMRI across cortical regions in humans. *Journal of Neuroscience*,

599   *31*, 12855–12865. https://doi.org/10.1523/JNEUROSCI.1457-11.2011

600   Conner, C. R., Kadipasaoglu, C. M., Shouval, H. Z., Hickok, G., & Tandon, N. (2019). Network dynamics of

601   Broca's area during word selection. *PLoS ONE*, *14*(12), 1–30. https://doi.org/10.1371/journal.pone.0225756

602   Cox, R. W. (1996). AFNI: Software for Analysis and Visualization of Functional Magnetic Resonance

603   Neuroimages. *Computers and Biomedical Research*, *29*(3), 162–173.

604   https://doi.org/10.1006/cbmr.1996.0014

605   Dale, A. M., Fischl, B., & Sereno, M. I. (1999). Cortical Surface-Based Analysis: I. Segmentation and Surface

606   Reconstruction. *NeuroImage*, *9*(2), 179–194. https://doi.org/10.1006/nimg.1998.0395

607   Davis, C. P., & Yee, E. (2019). Features, labels, space, and time: factors supporting taxonomic relationships in

608   the anterior temporal lobe and thematic relationships in the angular gyrus. *Language, Cognition and*

609   *Neuroscience*, *34*(10), 1347–1357.

610   Davis, Z. W., Muller, L., Martinez-Trujillo, J., Sejnowski, T., & Reynolds, J. H. (2020). Spontaneous travelling

611   cortical waves gate perception in behaving primates. *Nature*, *587*(7834), 432–436.

612   https://doi.org/10.1038/s41586-020-2802-y

613   Ding, N., Melloni, L., Zhang, H., Tian, X., & Poeppel, D. (2016). Cortical tracking of hierarchical linguistic

614   structures in connected speech. *Nature Neuroscience*, *19*(1), 158–164. https://doi.org/10.1038/nn.4186

615   Duffau, H., Moritz-Gasser, S., & Mandonnet, E. (2014). A re-examination of neural basis of language processing:

616   Proposal of a dynamic hodotopical model from data provided by brain stimulation mapping during picture

617   naming. *Brain and Language*, *131*, 1–10. https://doi.org/10.1016/j.bandl.2013.05.011

618   Fedorenko, E., Scott, T. L., Brunner, P., Coon, W. G., Pritchett, B., Schalk, G., & Kanwisher, N. (2016). Neural

619   correlate of the construction of sentence meaning. *Proceedings of the National Academy of Sciences of the*

620   *United States of America*, *113*(41), E6256–E6262. https://doi.org/10.1073/pnas.1612132113

621   Feng, X., Altarelli, I., Monzalvo, K., Ding, GuoshengRamus, F., Shu, H., Dehaene, S., … Dehaene-Lambertz, G.

622   (2020). A universal reading network and its modulation by writing system and reading ability in French and

623   Chinese children. *ELife*, *9*, e54591.

624   Figley, T. D., Mortazavi Moghadam, B., Bhullar, N., Kornelsen, J., Courtney, S. M., & Figley, C. R. (2017).

625   Probabilistic white matter atlases of human auditory, basal ganglia, language, precuneus, sensorimotor,

626   visual and visuospatial networks. *Frontiers in Human Neuroscience*, *11*(June), 1–12.

627   https://doi.org/10.3389/fnhum.2017.00306

628   Fischl, B., Sereno, M. I., & Dale, A. M. (1999). Cortical surface-based analysis: II. Inflation, flattening, and a

629   surface-based coordinate system. *NeuroImage*, *9*, 195–207. https://doi.org/10.1006/nimg.1998.0396

630   Flick, G., Oseki, Y., Kaczmarek, A. R., Al Kaabi, M., Marantz, A., & Pylkkänen, L. (2018). Building words and

631   phrases in the left temporal lobe. *Cortex*, *106*, 213–236. https://doi.org/10.1016/j.cortex.2018.06.004

632   Flick, G., & Pylkkänen, L. (2020). Isolating syntax in natural language: MEG evidence for an early contribution of

633   left posterior temporal cortex. *Cortex*, *127*, 42–57. https://doi.org/10.1016/j.cortex.2020.01.025

634   Flinker, A., Chang, E. F., Barbaro, N. M., Berger, M. S., & Knight, R. T. (2011). Sub-centimeter language

635   organization in the human temporal lobe. *Brain and Language*, *117*(3), 103–109.

636   https://doi.org/10.1016/j.bandl.2010.09.009

637   Forseth, K. J., Kadipasaoglu, C. M., Conner, C. R., Hickok, G., Knight, R. T., & Tandon, N. (2018). A lexical

638   semantic hub for heteromodal naming in middle fusiform gyrus. *Brain*, *141*(7), 2112–2126.

639   https://doi.org/10.1093/brain/awy120

640   Friederici, A. D., Chomsky, N., Berwick, R. C., Moro, A., & Bolhuis, J. J. (2017). Language, mind and brain.

641   *Nature Human Behaviour*, *1*(10), 713–722. https://doi.org/10.1038/s41562-017-0184-4

642   Fries, P. (2015). Rhythms for Cognition: Communication through Coherence. *Neuron*, *88*, 220–235.

643   https://doi.org/10.1016/j.neuron.2015.09.034

644   Gastaldon, S., Arcara, G., Navarrete, E., & Peressotti, F. (2020). Commonalities in alpha and beta neural

645   desynchronizations during prediction in language comprehension and production. *Cortex*, *133*, 328–345.

646   https://doi.org/10.1016/j.cortex.2020.09.026

647   Glasser, M. F., Coalson, T. S., Robinson, E. C., Hacker, C. D., Harwell, J., Yacoub, E., … Van Essen, D. C.

648   (2016). A multi-modal parcellation of human cerebral cortex. *Nature*, *536*(7615), 171–178.

649   https://doi.org/10.1038/nature18933

650   Glasser, M. F., & Rilling, J. K. (2008). DTI Tractography of the Human Brain's Language Pathways. *Cerebral*

651   *Cortex*, *18*(11), 2471–2482. https://doi.org/10.1093/cercor/bhn011

652   Graessner, A., Zaccarella, E., & Hartwigsen, G. (2021). Differential contributions of left-hemispheric language

653   regions to basic semantic composition. *Brain Structure and Function*. https://doi.org/10.1007/s00429-020-

654   02196-2

655   Hagoort, P. (2003). How the brain solves the binding problem for language: A neurocomputational model of

656   syntactic processing. *NeuroImage*, *20*, S18–S29. https://doi.org/10.1016/j.neuroimage.2003.09.013

657   Hagoort, P. (2004). Integration of Word Meaning and World Knowledge in Language Comprehension. *Science*,

658   *304*(5669), 438–441. https://doi.org/10.1126/science.1095455

659   Hagoort, P. (2005). On Broca, brain, and binding: A new framework. *Trends in Cognitive Sciences*.

660   https://doi.org/10.1016/j.tics.2005.07.004

661   Hagoort, P. (2013). MUC (Memory, Unification, Control) and beyond. *Frontiers in Psychology*, *4*.

662   https://doi.org/10.3389/fpsyg.2013.00416

663   Hagoort, P. (2017). The core and beyond in the language-ready brain. *Neuroscience & Biobehavioral Reviews*,

664   *81*, 194–204. https://doi.org/10.1016/j.neubiorev.2017.01.048

665   Hagoort, P. (2020). The meaning-making mechanism(s) behind the eyes and between the ears. *Philosophical*

666   *Transactions of the Royal Society of London. Series B, Biological Sciences*, *375*(1791), 20190301.

667   https://doi.org/10.1098/rstb.2019.0301

668   Hagoort, P., Baggio, G., & Willems, R. M. (2009). Semantic unification. In M. S. Gazzaniga (Ed.), *The Cognitive*

669   *Neurosciences* (4th ed., pp. 819–836). MIT Press.

670   Hagoort, P., & Indefrey, P. (2014). The Neurobiology of Language Beyond Single Words. *Annual Review of*

671   *Neuroscience*, *37*(1), 347–362. https://doi.org/10.1146/annurev-neuro-071013-013847

672   Hovsepyan, S., Olasagasti, I., & Giraud, A.-L. (2020). Combining predictive coding and neural oscillations

673   enables online syllable recognition in natural speech. *Nature Communications*, *11*(1), 3117.

674   https://doi.org/10.1038/s41467-020-16956-5

675   Humphries, C., Binder, J. R., Medler, D. A., & Liebenthal, E. (2006). Syntactic and semantic modulation of neural

676   activity during auditory sentence comprehension. *Journal of Cognitive Neuroscience*.

677   https://doi.org/10.1162/jocn.2006.18.4.665

678   Irimia, A., Van Horn, J. D., & Halgren, E. (2012). Source cancellation profiles of electroencephalography and

679   magnetoencephalography. *NeuroImage*, *59*(3), 2464–2474.

680   https://doi.org/10.1016/j.neuroimage.2011.08.104

681   Jackendoff, R., & Audring, J. (2020). *The Texture of the Lexicon: Relational Morphology and the Parallel*

682   *Architecture*. Oxford: Oxford University Press.

683   Jensen, O., Spaak, E., & Zumer, J. M. (2019). Human brain oscillations: From physiological mechanisms to

684   analysis and cognition. In *Magnetoencephalography: From Signals to Dynamic Cortical Networks: Second*

685   *Edition*. https://doi.org/10.1007/978-3-030-00087-5_17

686   Johnson, E. L., Kam, J. W. Y., Tzovara, A., & Knight, R. T. (2020). Insights into human cognition from intracranial

687   EEG: A review of audition, memory, internal cognition, and causality. *Journal of Neural Engineering*, *17*(5),

688   051001. https://doi.org/10.1088/1741-2552/abb7a5

689   Kadipasaoglu, C. M., Baboyan, V. G., Conner, C. R., Chen, G., Saad, Z. S., & Tandon, N. (2014). Surface-based

690   mixed effects multilevel analysis of grouped human electrocorticography. *NeuroImage*, *101*, 215–224.

691   https://doi.org/10.1016/j.neuroimage.2014.07.006

692   Kadipasaoglu, Cihan M., Forseth, K., Whaley, M., Conner, C. R., Rollo, M. J., Baboyan, V. G., & Tandon, N.

693   (2015). Development of grouped icEEG for the study of cognitive processing. *Frontiers in Psychology*,

694   *6*(1008). https://doi.org/10.3389/fpsyg.2015.01008

695   Keitel, A., Gross, J., & Kayser, C. (2018). Perceptually relevant speech tracking in auditory and motor cortex

696   reflects distinct linguistic features. *PLOS Biology*, *16*(3), e2004473.

697   https://doi.org/10.1371/journal.pbio.2004473

698   Keitel, A., Ince, R. A. A., Gross, J., & Kayser, C. (2017). Auditory cortical delta-entrainment interacts with

699   oscillatory power in multiple fronto-parietal networks. *NeuroImage*, *147*, 32–42.

700   https://doi.org/10.1016/j.neuroimage.2016.11.062

701   Kleiner, M., Brainard, D., Pelli, D., Ingling, A., Murray, R., & Broussard, C. (2007). What's new in psychtoolbox-3.

702   *Perception*, *36*(14), 1–16.

703   Kucyi, A., & Parvizi, J. (2020). Pupillary Dynamics Link Spontaneous and Task-Evoked Activations Recorded

704   Directly from Human Insula. *The Journal of Neuroscience*, *40*(32), 6207–6218.

705   https://doi.org/10.1523/JNEUROSCI.0435-20.2020

706   Lambon Ralph, M. A., Ehsan, S., Baker, G. A., & Rogers, T. T. (2012). Semantic memory is impaired in patients

707   with unilateral anterior temporal lobe resection for temporal lobe epilepsy. *Brain*, *135*(1), 242–258.

708   https://doi.org/10.1093/brain/awr325

709   Lau, E., Stroud, C., Plesch, S., & Phillips, C. (2006). The role of structural prediction in rapid syntactic analysis.

710   *Brain and Language*, *98*(1), 74–88. https://doi.org/10.1016/j.bandl.2006.02.003

711   Law, R., & Pylkkänen, L. (2021). Lists with and without Syntax: A New Approach to Measuring the Neural

712   Processing of Syntax. *The Journal of Neuroscience*, *41*(10), 2186–2196.

713   https://doi.org/10.1523/JNEUROSCI.1179-20.2021

714   Lee, D. K., Fedorenko, E., Simon, M. V., Curry, W. T., Nahed, B. V., Cahill, D. P., & Williams, Z. M. (2018).

715   Neural encoding and production of functional morphemes in the posterior temporal lobe. *Nature*

716   *Communications*, *9*, 1877. https://doi.org/10.1038/s41467-018-04235-3

717   Leivada, E., & Murphy, E. (2021). Mind the (terminological) gap: 10 misused, ambiguous, or polysemous terms in

718   linguistics. *Ampersand*, *8*, 100073. https://doi.org/10.1016/j.amper.2021.100073

719   Leszczyński, M., Barczak, A., Kajikawa, Y., Ulbert, I., Falchier, A. Y., Tal, I., … Schroeder, C. E. (2020).

720   Dissociation of broadband high-frequency activity and neuronal firing in the neocortex. *Science Advances*,

721   *6*(33), eabb0977. https://doi.org/10.1126/sciadv.abb0977

722   Lewis, A. G., Schoffelen, J.-M., Schriefers, H., & Bastiaansen, M. (2016). A Predictive Coding Perspective on

723   Beta Oscillations during Sentence-Level Language Comprehension. *Frontiers in Human Neuroscience*, *10*,

724   83. https://doi.org/10.3389/fnhum.2016.00085

725   Lopopolo, A., van den Bosch, A., Petersson, K.-M., & Willems, R. M. (2021). Distinguishing Syntactic Operations

726   in the Brain: Dependency and Phrase-Structure Parsing. *Neurobiology of Language*, *2*(1), 152–175.

727   https://doi.org/10.1162/nol_a_00029

728   Mai, G., Minett, J. W., & Wang, W. S.-Y. (2016). Delta, theta, beta, and gamma brain oscillations index levels of

729   auditory sentence processing. *NeuroImage*, *133*, 516–528.

730   https://doi.org/10.1016/j.neuroimage.2016.02.064

731   Marko, M., Cimrová, B., & Riečanský, I. (2019). Neural theta oscillations support semantic memory retrieval.

732   *Scientific Reports*, *9*(1), 17667. https://doi.org/10.1038/s41598-019-53813-y

733   Marple, L. (1999). Computing the discrete-time "analytic" signal via FFT. *IEEE Transactions on Signal*

734   *Processing*, *47*(9), 2600–2603.

735   Martin, S., Millán, J. del R., Knight, R. T., & Pasley, B. N. (2019). The use of intracranial recordings to decode

736   human language: Challenges and opportunities. *Brain and Language*, *193*, 73–83.

737   https://doi.org/10.1016/j.bandl.2016.06.003

738   Matar, S., Dirani, J., Marantz, A., & Pylkkänen, L. (2021). Left posterior temporal cortex is sensitive to syntax

739   within conceptually matched Arabic expressions. *Scientific Reports*, *11*(7181).

740   Matchin, W., & Hickok, G. (2020). The Cortical Organization of Syntax. *Cerebral Cortex*, *30*(3), 1481–1498.

741   https://doi.org/10.1093/cercor/bhz180

742   Muller, L., Chavane, F., Reynolds, J., & Sejnowski, T. J. (2018). Cortical travelling waves: mechanisms and

743   computational principles. *Nature Reviews Neuroscience*, *19*(5), 255–268.

744   https://doi.org/10.1038/nrn.2018.20

745   Murphy, E. (2015a). Labels, cognomes, and cyclic computation: An ethological perspective. *Frontiers in*

746   *Psychology*, *6*(715). https://doi.org/10.3389/fpsyg.2015.00715

747   Murphy, E. (2015b). The brain dynamics of linguistic computation. *Frontiers in Psychology*, *6*(1515).

748   https://doi.org/10.3389/fpsyg.2015.01515

749   Murphy, Elliot. (2015). Labels, cognomes, and cyclic computation: An ethological perspective. *Frontiers in*

750   *Psychology*, *6*(715). https://doi.org/10.3389/fpsyg.2015.00715

751   Murphy, Elliot. (2018). Interfaces (travelling oscillations) + recursion (delta-theta code) = language. In E. Luef &

752   M. Manuela (Eds.), *The Talking Species: Perspectives on the Evolutionary, Neuronal and Cultural*

753   *Foundations of Language* (pp. 251–269). Graz.

754   Murphy, Elliot. (2019). No Country for Oldowan Men: Emerging Factors in Language Evolution. *Frontiers in*

755   *Psychology*, *10*. https://doi.org/10.3389/fpsyg.2019.01448

756   Murphy, Elliot. (2020). *The Oscillatory Nature of Language*. Cambridge: Cambridge University Press.

757   Murphy, Elliot, Holmes, E., & Friston, K. (2021). Natural language syntax complies with the free-energy principle.

758   *PsyArXiv*. https://doi.org/doi.org/10.31234/osf.io/r3fcx

759   Murphy, Elliot, & Shim, J.-Y. (2020). Copy invisibility and (non-)categorial labeling. *Linguistic Research*, *37*(2),

760   187–215. https://doi.org/10.17250/khisli.37.2.202006.002

761   Nelson, M. J., El Karoui, I., Giber, K., Yang, X., Cohen, L., Koopman, H., … Dehaene, S. (2017).

762   Neurophysiological dynamics of phrase-structure building during sentence processing. *Proceedings of the*

763   *National Academy of Sciences of the United States of America*, *114*(18), E3669–E3678.

764   https://doi.org/10.1073/pnas.1701590114

765   Neufeld, C., Kramer, S. E., Lapinskaya, N., Heffner, C. C., Malko, A., & Lau, E. F. (2016). The electrophysiology

766   of basic phrase building. *PLoS ONE*, *11*(10), 1–22. https://doi.org/10.1371/journal.pone.0158446

767   Packard, P. A., Steiger, T. K., Fuentemilla, L., & Bunzeck, N. (2020). Neural oscillations and event-related

768   potentials reveal how semantic congruence drives long-term memory in both young and older humans.

769   *Scientific Reports*. https://doi.org/10.1038/s41598-020-65872-7

770   Pieters, T. A., Conner, C. R., & Tandon, N. (2013). Recursive grid partitioning on a cortical surface model: an

771   optimized technique for the localization of implanted subdural electrodes. *Journal of Neurosurgery*, *118*(5),

772   1086–1097. https://doi.org/10.3171/2013.2.JNS121450

773   Pietroski, P. M. (2018). Conjoining meanings: Semantics without truth values. In *Conjoining Meanings: Semantics*

774   *Without Truth Values*. https://doi.org/10.1093/oso/9780198812722.001.0001

775   Pobric, G., Jefferies, E., & Lambon Ralph, M. A. (2010). Category-Specific versus Category-General Semantic

776   Impairment Induced by Transcranial Magnetic Stimulation. *Current Biology*, *20*(10), 964–968.

777   https://doi.org/10.1016/j.cub.2010.03.070

778   Prystauka, Y., & Lewis, A. G. (2019). The power of neural oscillations to inform sentence comprehension: A

779   linguistic perspective. *Language and Linguistics Compass*, *13*(9). https://doi.org/10.1111/lnc3.12347

780   Pulvermüller, F., & Grisoni, L. (2020). Semantic prediction in brain and mind. *Trends in Cognitive Sciences*,

781   *24*(10), 781–784.

782   Pylkkänen, L. (2020). Neural basis of basic composition: what we have learned from the red-boat studies and

783   their extensions. *Philosophical Transactions of the Royal Society of London. Series B, Biological Sciences*,

784   *375*(1791), 20190299. https://doi.org/10.1098/rstb.2019.0299

785   Pylkkänen, L., & Brennan, J. (2020). Composition: the neurobiology of syntactic and semantic phrase structure

786   building. In D. Poeppel, G. . Mangun, & M. . Gazzaniga (Eds.), *The Cognitive Neurosciences* (6th ed.).

787   Cambridge, MA: MIT Press.

788   Rizzi, L. (2016). Monkey morpho-syntax and merge-based systems. *Theoretical Linguistics*, *42*(1–2), 139–145.

789   https://doi.org/10.1515/tl-2016-0006

790   Rollo, P. S., Rollo, M. J., Zhu, P., Woolnough, O., & Tandon, N. (2020). Oblique trajectory angles in robotic

791   stereo-electroencephalography. *Journal of Neurosurgery*, 1–10. https://doi.org/10.3171/2020.5.JNS20975

792   Saad, Z. S., & Reynolds, R. C. (2012). SUMA. *NeuroImage*, *62*, 768–773.

793   https://doi.org/10.1016/j.neuroimage.2011.09.016

794   Sarubbo, S., Tate, M., De Benedictis, A., Merler, S., Moritz-Gasser, S., Herbet, G., & Duffau, H. (2020). Mapping

795   critical cortical hubs and white matter pathways by direct electrical stimulation: an original functional atlas of

796   the human brain. *NeuroImage*, *205*(September 2019), 116237.

797   https://doi.org/10.1016/j.neuroimage.2019.116237

798   Sauseng, P., & Klimesch, W. (2008). What does phase information of oscillatory brain activity tell us about

799   cognitive processes? *Neuroscience and Biobehavioral Reviews*, *32*, 1001–1013.

800   https://doi.org/10.1016/j.neubiorev.2008.03.014

801   Schell, M., Zaccarella, E., & Friederici, A. D. (2017). Differential cortical contribution of syntax and semantics: An

802   fMRI study on two-word phrasal processing. *Cortex*, *96*, 105–120.

803   https://doi.org/10.1016/j.cortex.2017.09.002

804   Segaert, K., Mazaheri, A., & Hagoort, P. (2018). Binding language: structuring sentences through precisely timed

805   oscillatory mechanisms. *European Journal of Neuroscience*, *48*(7), 2651–2662.

806   https://doi.org/10.1111/ejn.13816

807   Tandon, N. (2012). Mapping of human language. In D. Yoshor & E. Mizrahi (Eds.), *Clinical Brain Mapping* (pp.

808   203–218). McGraw Hill Education.

809   Tandon, N., Tong, B. A., Friedman, E. R., Johnson, J. A., Von Allmen, G., Thomas, M. S., … Thompson, S. A.

810   (2019). Analysis of Morbidity and Outcomes Associated with Use of Subdural Grids vs

811   Stereoelectroencephalography in Patients with Intractable Epilepsy. *JAMA Neurology*, *76*, 672–681.

812   https://doi.org/10.1001/jamaneurol.2019.0098

813   Tanji, K., Suzuki, K., Delorme, A., Shamoto, H., & Nakasato, N. (2005). High-frequency γ-band activity in the

814   basal temporal cortex during picture-naming and lexical-decision tasks. *Journal of Neuroscience*, *25*(13),

815   3287–3293. https://doi.org/10.1523/JNEUROSCI.4948-04.2005

816   Terporten, R., Schoffelen, J. M., Dai, B., Hagoort, P., & Kösem, A. (2019). The Relation between Alpha/Beta

817   Oscillations and the Encoding of Sentence induced Contextual Information. *Scientific Reports*.

818   https://doi.org/10.1038/s41598-019-56600-x

819   Thye, M., Geller, J., Szaflarski, J. P., & Mirman, D. (2021). Intracranial EEG evidence of functional specialization

820   for taxonomic and thematic relations. *Cortex*. https://doi.org/10.1016/j.cortex.2021.03.018

821   Tong, B. A., Esquenazi, Y., Johnson, J., Zhu, P., & Tandon, N. (2020). The Brain is Not Flat: Conformal Electrode

822   Arrays Diminish Complications of Subdural Electrode Implantation, A Series of 117 Cases. *World*

823   *Neurosurgery*, *144*, e734–e742. https://doi.org/10.1016/j.wneu.2020.09.063

824   Towle, V. L., Yoon, H.-A., Castelle, M., Edgar, J. C., Biassou, N. M., Frim, D. M., … Kohrman, M. H. (2008).

825   ECoG gamma activity during a language task: differentiating expressive and receptive speech areas. *Brain*,

826   *131*(8), 2013–2027. https://doi.org/10.1093/brain/awn147

827   Trettenbrein, P., Papitto, G., Friederici, A. D., & Zaccarella, E. (2020). Functional neuroanatomy of language

828   without speech: An ALE meta-analysis of sign language. *Human Brain Mapping*, *doi.org/10*.

829   Wang, X., Men, W., Gao, J., Caramazza, A., & Bi, Y. (2020). Two Forms of Knowledge Representations in the

830   Human Brain. *Neuron*, *107*(2), 383–393. https://doi.org/10.1016/j.neuron.2020.04.010

831   Westerlund, M., Kastner, I., Al Kaabi, M., & Pylkkänen, L. (2015). The LATL as locus of composition: MEG

832   evidence from English and Arabic. *Brain and Language*, *141*, 124–134.

833   https://doi.org/10.1016/j.bandl.2014.12.003

834   Westerlund, M., & Pylkkänen, L. (2014). The role of the left anterior temporal lobe in semantic composition vs.

835   semantic memory. *Neuropsychologia*, *57*(1), 59–70.

836   https://doi.org/10.1016/j.neuropsychologia.2014.03.001

837   Wilson, S. M., DeMarco, A. T., Henry, M. L., Gesierich, B., Babiak, M., Mandelli, M. L., … Gorno-Tempini, M. L.

838   (2014). What role does the anterior temporal lobe play in sentence-level processing? neural correlates of

839   syntactic processing in semantic variant primary progressive aphasia. *Journal of Cognitive Neuroscience*,

840   *26*(5), 970–985. https://doi.org/10.1162/jocn_a_00550

841   Wilson, S. M., & Saygin, A. P. (2004). Grammaticality Judgment in Aphasia: Deficits Are Not Specific to Syntactic

842   Structures, Aphasic Syndromes, or Lesion Sites. *Journal of Cognitive Neuroscience*, *16*, 238–252.

843   https://doi.org/10.1162/089892904322984535

844   Woolnough, O., Forseth, K. J., Rollo, P. S., & Tandon, N. (2019). Uncovering the functional anatomy of the

845   human insula during speech. *ELife*, *8*, 1–14. https://doi.org/10.7554/eLife.53086

846   Yi, H. G., Leonard, M. K., & Chang, E. F. (2019). The Encoding of Speech Sounds in the Superior Temporal

847   Gyrus. *Neuron*, *102*(6), 1096–1110. https://doi.org/10.1016/j.neuron.2019.04.023

848   Zaccarella, E., Papitto, G., & Friederici, A. D. (2021). Language and action in Broca's area: Computational

849   differentiation and cortical segregation. *Brain and Cognition*, *147*, 105651.

850   https://doi.org/10.1016/j.bandc.2020.105651

851   Zhang, L., & Pylkkänen, L. (2018). Semantic composition of sentences word by word: MEG evidence for shared

852   processing of conceptual and logical elements. *Neuropsychologia*, *119*(April), 392–404.

853   https://doi.org/10.1016/j.neuropsychologia.2018.08.016

854

855   **Supplementary Figures**
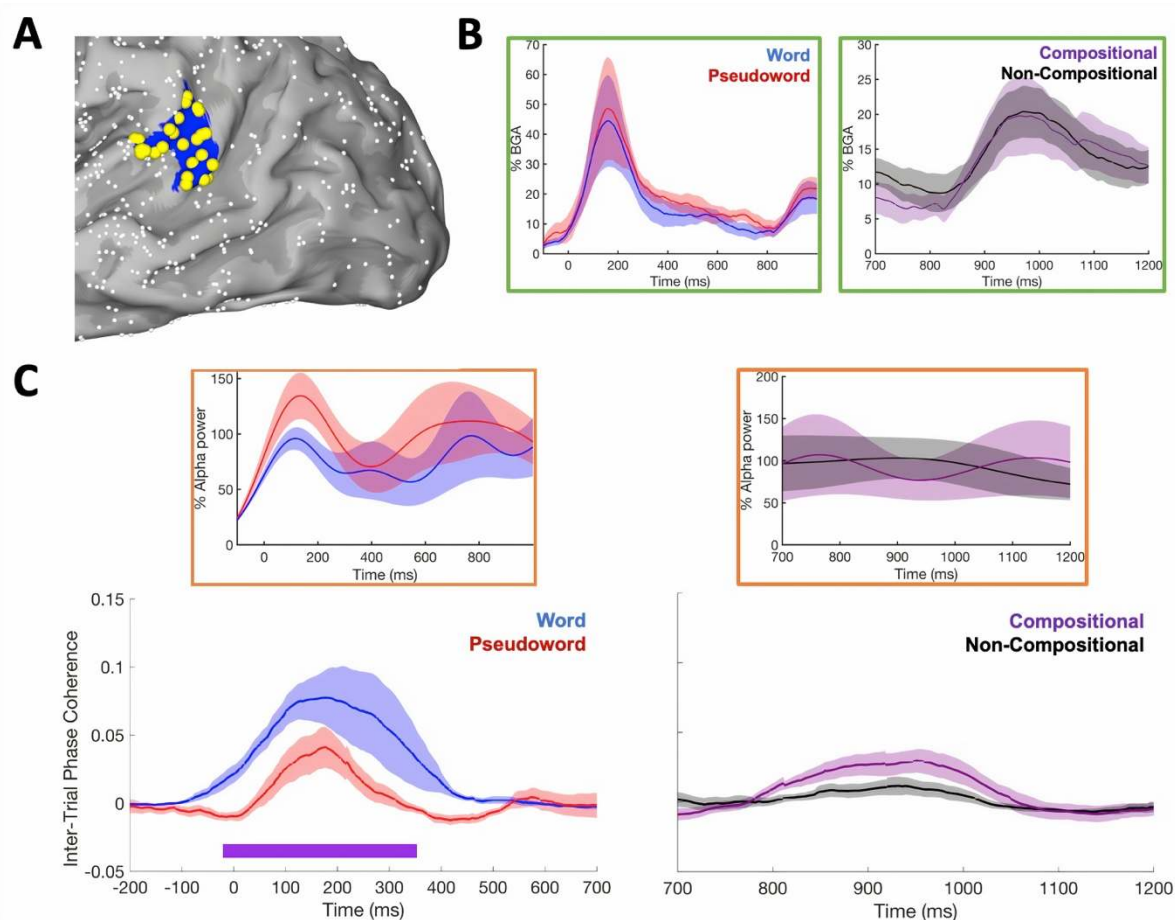
856

857   <u>**Supplementary Figure 1**</u>: **Inter-trial phase coherence and lexicality.**

858   (A) Electrodes with significant differences in ITC for words vs pseudowords, in a portion of
859   posterior temporal cortex with a high concentration of electrodes exhibiting significant
860   differences (9 patients); HCP index: area STV (Glasser et al., 2016). (B) Gamma traces (green
861   dashed box) for electrodes in (A) for words vs. pseudowords and compositional vs. non-
862   compositional trials (C) ITC in alpha (8-12Hz) for all electrodes in (A) for words (blue) and
863   pseudowords (red) on the left, with alpha (orange dashed box) amplitude traces, and for
864   phrase composition (purple) and non-composition (black) on the right isolated around the
865   onset of the second word (no significant effect for composition contrast). T0 = first word onset.

866

33
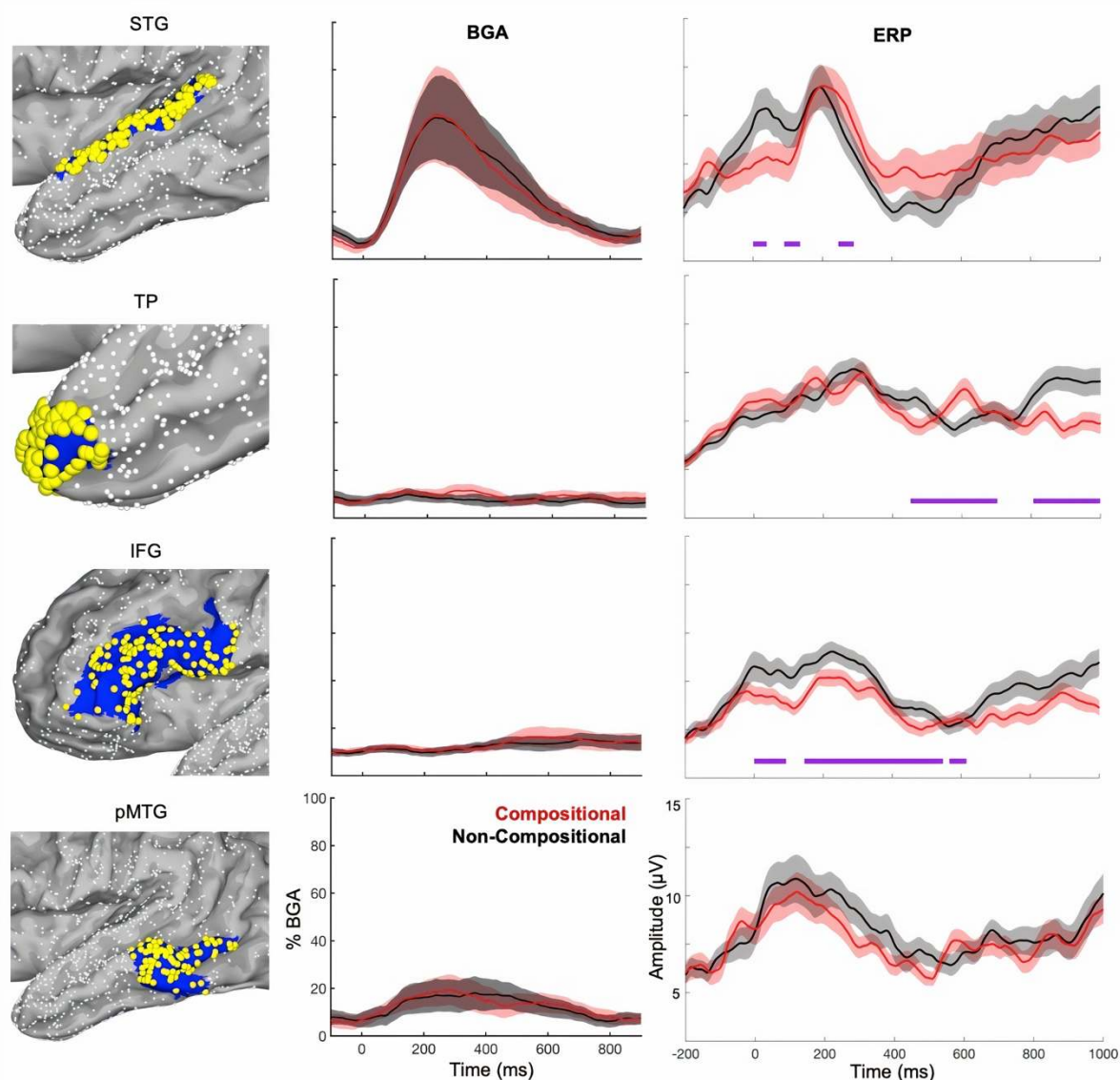
Supplementary Figure 2: **Regions of interest and their BGA/ERP signatures.** Regional broadband gamma amplitude (middle column) with event-related potentials (right column). Red: Compositional. Black: Non-Compositional. HCP index from top-down: posterior superior temporal gyrus (pSTG) = [A4]; temporal pole = [TGd]; inferior frontal gyrus (IFG) = [FOP4, 44, 45, IFSp, p47r, IFSa, 47l]; posterior middle temporal gyrus (pMTG) = [PHT, TE1p]. BGA traces are thresholded by p<0.05 significantly active from baseline (first word onset, -500 to -100ms) with a minimum of 10% BGA amplitude increase during the 100-400ms post-second word onset period. ERPs were computed across the four ROIs plotted on the left column, with significant condition differences being computed across 0-1000ms in the same (FDR-corrected) manner as the BGA plots (see Methods).
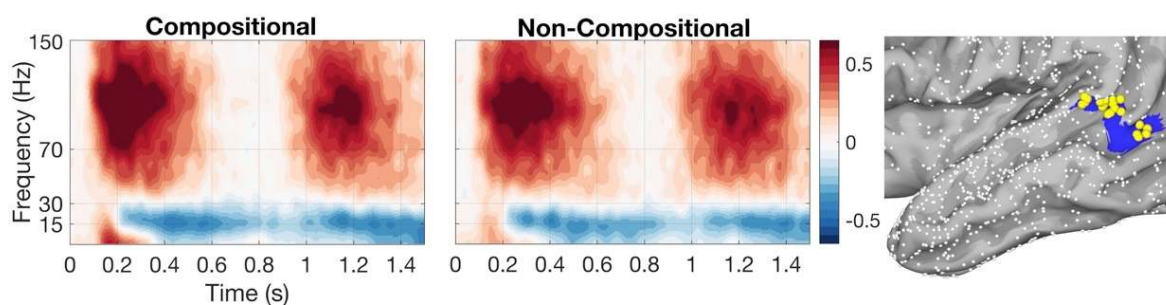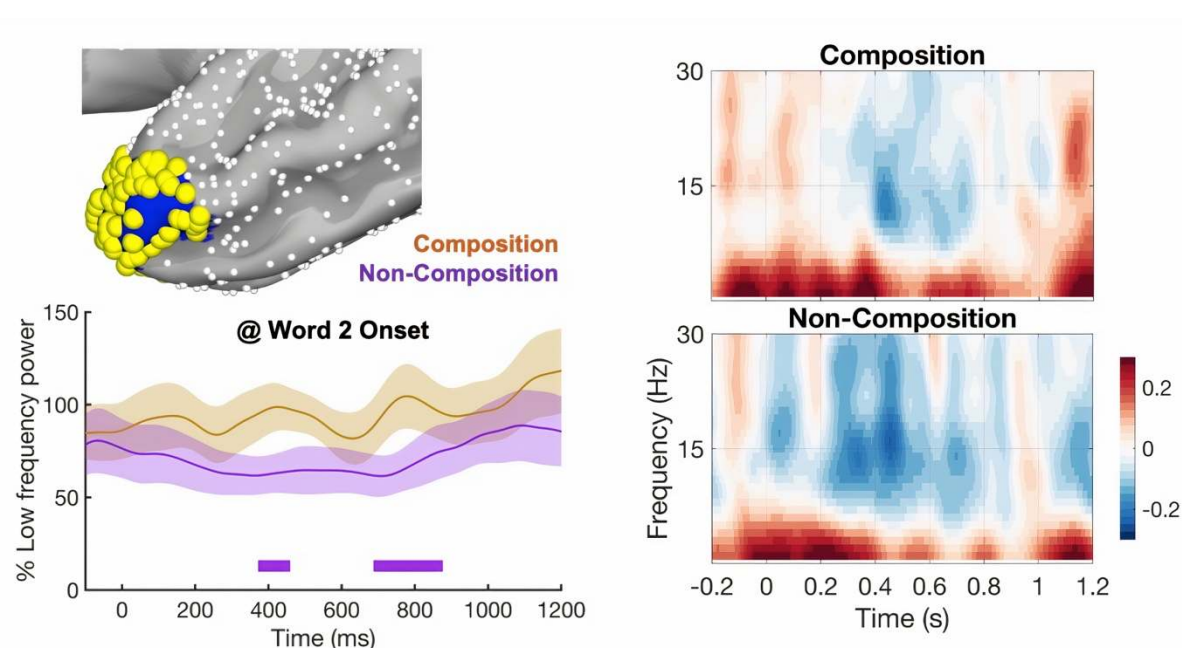
Supplementary Figure 3: **pSTS-TOJ regional spectrograms.** Spectrograms and electrodes in pSTS-TOJ for all active channels (HCP index: TPOJ1; electrodes = 23, patients = 10). Second word onset was at 800ms.

Supplementary Figure 4: **Temporal pole effects.** Low frequency (2–15Hz) temporal pole trace with FDR-significant bars for the Compositional (brown) vs Non-Compositional (purple) contrast (HCP index: TGd) with spectrograms, thresholded at 10% increased activity from baseline; T0 = second word onset. For BGA, see Suppl. Fig. 2.